REFERENCES

Bernhardt, H., Hoyer, O., Schell, H. & Lusse, B. 1985 Reaction mechanisms involved in the influence of algogenic organic matter on flocculation. *Z. Wasser Abwass. For.* **18**(1), 18–30.

Binnie, C., Kimber, M. & Smethurst, G. 2002 *Basic Water Treatment*, 3rd edition. Thomas Telford, London.

Gregory, D. & Carlson, K. 2003 Relationship of pH and floc formation kinetics to granular media filtration performance. *Environ. Sci. Technol.* **37**, 1398–1403.

Hayashi, C. 1950 On the quantification of qualitative data from the mathematico-statistical point of view. *Ann. Inst. Stat. Math.* **2**, 35–47.

Hayashi, C. 1952 On the prediction of phenomena from qualitative data and the quantification of qualitative data from the mathematico-statistical point of view. *Ann. Inst. Stat. Math.* **3**, 69–98.

Japan Water Works Association (JWWA) 2000 *Design Criteria for Waterworks Facilities*. Japan Water Works Association, Tokyo (in Japanese).

JWWA 2001 *Japanese Standard Methods for the Examination of Water*. Japan Water Works Association, Tokyo (in Japanese), pp. 134–136.

JWWA 2003 *Suidou Toukei (Statistics on Water Supply)*. Vol. 84. Japan Water Works Association, Tokyo (in Japanese).

JWWA 2004 *Statistics on Water Supply*. Vol. 85. Japan Water Works Association, Tokyo (in Japanese).

JWWA 2005 *Statistics on Water Supply*. Vol. 86. Japan Water Works Association, Tokyo (in Japanese).

JWWA 2006 *Statistics on Water Supply*. Vol. 87. Japan Water Works Association, Tokyo (in Japanese).

JWWA 2007*a* Analyses across the years with statistics on water supply of fiscal year 2005. *J. Jpn Water Works Assoc.* **76**(9), 88–126 (in Japanese).

JWWA 2007*b* *Statistics on Water Supply*. Vol. 88. Japan Water Works Association, Tokyo (in Japanese).

MWH 2005 *Water Treatment: Principles and Design*, 2nd edition. John Wiley & Sons, New York, pp. 676–679.

National Research Council (NRC) 1997 *Safe Water from Every Tap: Improving Water Service to Small Communities*. National Academy Press, Washington, DC.

Ogasawara, K. 2008 Challenges for small water utilities and their direction to the future. *Suido* **53**(3), 1–18 (in Japanese).

Pivokonsky, M., Kloucek, O. & Pivokonska, L. 2006 Evaluation of the production, composition and aluminum and iron complexation of algogenic organic matter. *Water Res.* **40**(16), 3045–3052.

Qin, J. J., Oo, M. H., Kekre, K. A., Knops, F. & Miller, P. 2006 Impact of coagulation pH on enhanced removal of natural organic matter in treatment of reservoir water. *Sep. Sci. Technol.* **49**, 295–298.

Takaara, T., Sano, D., Konno, H. & Omura, T. 2005 Affinity isolation of algal organic matters able to form complex with aluminium coagulant. *Water Sci. Technol. Water Supply* **4**(5–6), 95–102.

Takaara, T., Sano, D., Konno, H. & Omura, T. 2007 Cellular proteins of microcystis aeruginosa inhibiting coagulation with polyaluminum chloride. *Water Res.* **41**(8), 1653–1658.

Tambo, N. 1980 *Water Supply System: New System of Civil Engineering 88*. Gihodoshuppan, Tokyo (in Japanese).

World Health Organization (WHO) 2004 *Guidelines for Drinking-Water Quality*, 3rd edition. (Vol. 1). World Health Organization, Geneva, pp. 301–303.

Yan, M., Wang, D., Ni, J., Qu, J., Chow, C. W. K. & Liu, H. 2008 Mechanism of natural organic matter removal by polyaluminum chloride: effect of coagulant particle size and hydrolysis kinetics. *Water Res.* **42**, 3361–3370.

First received 1 October 2008; accepted in revised form 30 July 2009

WATER RESEARCH 43 (2009) 5160–5170

Available at www.sciencedirect.com

ScienceDirect

journal homepage: www.elsevier.com/locate/watres

Effects of super-powdered activated carbon pretreatment on coagulation and trans-membrane pressure buildup during microfiltration

Yoshihiko Matsui [a,*], Hiroki Hasegawa [a], Koich Ohno [a], Taku Matsushita [a], Satoru Mima [b], Yuji Kawase [b], Takako Aizawa [c]

[a] Graduate School of Engineering, Hokkaido University, N13W8, Sapporo 060-8628, Japan
[b] Metawater Co. Ltd., Toranomon 4-3-1, Minato-ku, Tokyo 105-6029, Japan
[c] Japan Water Research Center, Toranomon2-8-1, Minato-ku, Tokyo, 105-0001, Japan

ARTICLE INFO

Article history:
Received 6 July 2009
Received in revised form
13 August 2009
Accepted 14 August 2009
Available online 26 August 2009

Keywords:
Membrane fouling
Membrane permeability
Powdered activated carbon
Pretreatment
Flocculation
Floc

ABSTRACT

As a pretreatment for membrane microfiltration (MF), the use of powdered activated carbon (PAC) with a particle size much smaller than that of conventional PAC (super-powdered PAC, or S-PAC) has been proposed to enhance the removal of dissolved substances. In this paper, another advantage of S-PAC as a pretreatment for MF is described: the use of S-PAC attenuates trans-membrane pressure increases during the filtration operation. The floc particles that formed during coagulation preceded by S-PAC pretreatment were larger and more porous than the floc particles formed during coagulation preceded by PAC pretreatment and those formed during coagulation without pretreatment. This result was due to increased particle–particle collision frequency and better removal of natural organic matter, which inhibits coagulation by consuming coagulant, before the coagulation reaction. The caked fouling layer that built up on the membrane surface was thus more permeable with S-PAC than with normal PAC. Both physically reversible and irreversible membrane foulings were reduced, and more stable filtration was accomplished with S-PAC pretreatment.

© 2009 Elsevier Ltd. All rights reserved.

1. Introduction

Although water treatment systems that use low-pressure membrane technology (microfiltration, MF, and ultrafiltration, UF) have small footprints, completely separate suspended matter and bacteria, and require little maintenance and operational skill, they have disadvantages, such as energy consumption due to decreasing permeability caused by membrane fouling. In addition, dissolved substances such as disinfection byproducts and their precursors are not removed by this technology alone. The inability to remove dissolved substances is often addressed by pretreatment before filtration. Chemical coagulation and adsorption are the most popular pretreatments because they are inexpensive and are easy to use, and they have been extensively studied (Huang et al., 2009). A ferric or aluminum coagulant, powdered activated carbon (PAC) adsorbent, or both are added before membrane filtration (Mallevialle, 1996; Baudin et al., 2001),

* Corresponding author. Tel.: +81 11 706 7280.
E-mail addresses: matsui@eng.hokudai.ac.jp (Y. Matsui), h-hase@eng.hokudai.ac.jp (H. Hasegawa), ohnok@eng.hokudai.ac.jp (K. Ohno), taku-m@eng.hokudai.ac.jp (T. Matsushita), mima-satoru@metawater.co.jp (S. Mima), kawase-yuji@metawater.co.jp (Y. Kawase), aizawat@seaple.icc.ne.jp (T. Aizawa).
0043-1354/$ – see front matter © 2009 Elsevier Ltd. All rights reserved.
doi:10.1016/j.watres.2009.08.021

and the floc particles formed by coagulation and the PAC particles bearing the adsorbed dissolved substances are removed during membrane filtration.

Pretreatments reduce membrane fouling during filtration either by removing or modifying potential foulants (Carroll et al., 2000; Howe et al., 2006; Gray et al., 2008). For example, chemical coagulation aggregate particles and organic matter, and aggregation in turn limits pore blockage and enables the formation of a more porous cake that is easily removed by hydraulic cleaning (Laîné et al., 1989; Jack and Clark, 1998; Carroll et al., 2000; Park et al., 2002; Leiknes et al., 2004; Oh and Lee, 2005; Cho et al., 2005; Chen et al., 2007; Fan et al., 2008). Physically reversible membrane fouling caused by cake resistance on the membrane depends straightforwardly on the coagulation conditions. At higher coagulant doses, a more permeable cake forms, or protection of the membrane from foulants is greater (Judd and Hillis, 2001; Pikkarainen et al., 2004; Choi and Dempsey, 2004). In the case of dead-end filtration, the formation of a porous cake with large floc particles is a key, and the optimum conditions for the production of large flocs that are resistant enough to shear stress to facilitate flow between the aggregates have been quantified (Lee et al., 2000, 2005; Park et al., 2006, 2007; Barbot et al., 2008). In contrast, physically irreversible membrane fouling is more complex and depends not only on coagulation conditions but also on the membrane material and the filtration conditions, including the membrane cleaning method (Lahoussine-Turcaud et al., 1990; Kimura et al., 2008).

There has been some discussion about whether PAC itself fouls membranes as well as attenuating membrane permeability reduction (Yiantsios and Karabelas, 2001; Tomaszewska and Mozia, 2002). For example, Adham et al. (1991) reported that the addition of PAC to a UF process did not increase the rate of flux decline. Li and Chen (2004) reported that PAC pretreatment did not improve membrane permeability, because the fractions that were not adsorbed by PAC caused more fouling than the fractions that were adsorbed by PAC. The addition of PAC sometimes fouls the membrane, depending on the PAC–membrane interaction and the characteristics of the PAC cake-layer (Zhang et al., 2003; Mozia et al., 2005; Jang et al., 2006; Takizawa et al., 2008). However, the combination of chemical coagulation and PAC adsorption pretreatments has been shown to alleviate fouling (Jack and Clark, 1998; Haberkamp et al., 2007).

Due to the robustness of ceramic membranes, which allow high fluxes and rigorous cleaning methods, such membranes are increasingly being used as an alternative to polymeric membranes in the treatment of drinking water and wastewater. Ceramic membrane MF is becoming accepted for full-scale facilities, such as the 39,000 m^3/d Hinogawa Water Treatment Plant near Kyoto, Japan, where poly-aluminum chloride coagulation is followed by short-duration flocculation and direct monolith ceramic membrane MF (Kanaya et al., 2007). A monolith ceramic membrane plant with a much larger capacity (170,000 m^3/d) is being planned for Yokohama, Japan. Ceramic membrane MF processes are usually designed to include pretreatment with a hydrolyzing metal coagulant (e.g., poly-aluminum chloride) followed by direct MF in dead-end mode (Loi-Brügger et al., 2006). Operational data of pilot plants and actual facilities have shown that water treatment processes using a ceramic membrane and chemical coagulation pretreatment are stable for dead-end filtration, even without long-duration flocculation and sedimentation. Pilot plant experiments and flow analysis have proved that monolith ceramic membranes show a unique flow pattern in the channels within the monolith element, causing extremely rapid flocculation in the channels during dead-end filtration. Most of the flocculated particles form a columnar cake with high permeability at the dead-end point (Yonekawa et al., 2004).

For pretreatment in ceramic membrane MF, the use of activated carbon with a particle size much smaller than that of conventional PAC (super-PAC, or S-PAC) has been proposed to address the inability of the MF to remove dissolved substances (Matsui et al., 2004; Matsui et al., 2005). The small size of S-PAC, which enables faster adsorption kinetics (Matsui et al., 2009), enhances the adsorbate uptake rate over a limited retention time and thereby permits much shorter activated carbon–water contact times when used as a pretreatment for membrane filtration. Substantial enhancement of the adsorptive removal rate of geosmin has been achieved with S-PAC (Matsui et al.. 2007). The addition of S-PAC does not result in fouling of the membrane; in fact, it alleviates trans-membrane pressure (TMP) buildup in ceramic membrane MF. However, the filtration operation period of the reported experiments was relatively short, and the mechanism was not clearly explained. Therefore, further study is necessary to clarify the effect of S-PAC on TMP buildup in ceramic membrane MF with adsorption and coagulation pretreatments.

In this research, we conducted long-term pilot- and laboratory-scale experiments and compared the effects of S-PAC pretreatment, normal PAC pretreatment, and coagulation only (no PAC pretreatment) on the permeability of a ceramic membrane during MF. We also discuss the mechanism of the S-PAC pretreatment effects.

2. Materials and methods

2.1. *Pilot-scale MF system*

A small membrane filtration pilot plant within the Kawai Water Purification Plant at Yokohama, Japan, was used for the experiments. The plant has three parallel MF lines that can be operated independently under different operational conditions. Each line has a small membrane module containing a tubular, ceramic monolith membrane element (nominal pore size, 0.1 μm; filtration area, 0.4 m^2; 55 channels; membrane diameter, 30 mm; membrane length, 1 m; Metawater Co., Nagoya, Japan), which was designed for small-scale experiments. (The membrane element used for the full-scale filtration plant has a membrane surface area of 25 m^2, a diameter of 1800 mm, and a length of 1.5 m.) In the membrane filtration experiments, raw water from Lake Sagami (Kanagawa, Japan) was first introduced into the MF feed tank and then distributed to the MF lines after pH adjustment with diluted sulfuric acid. The S-PAC and PAC were added at inlets of the tube reactors at controlled dose rates. After contact with the adsorbent in the tube reactors,

the coagulant (poly-aluminum chloride, PACl, Hieisyouten Co., Aichi, Japan) was added. PACl, S-PAC and PAC dose rates were determined by referring to the previous MF experimental results (Matsui et al., 2007). The flow of feed to the membrane module was configured in dead-end mode at a constant rate (filtration rate, 3 m/d = 0.125 m/h) inside the module by positive pressure, the membranes were hydraulically backwashed periodically with the hypochlorite-injected membrane permeate at a pressure of 500 kPa, and the retentate was discharged by pressurized air.

2.2. *Laboratory-scale MF system*

Fig. 1 is a schematic diagram of the experimental setup for the laboratory-scale MF tests. Water was fed to the system by a peristaltic pump. Either S-PAC or PAC was added at the inlet of the tube reactor. After contact with the activated carbon, the water was transferred to a second tube reactor, where the PACl (10% Al_2O_3, Taki Chemical Co., Hyogo, Japan) was added after dilution with pure water (Milli-Q Advantage, Nihon Millipore K.K., Tokyo, Japan) by a factor of 1 in 59,000 (diluted PACl was prepared every day to avoid deterioration due to excessive hydrolysis). The ceramic membrane element was the same as that used in the pilot-scale system, except that all but one of the 55 channels was plugged with glue. Filtration occurred at a constant flow rate (2 m/d = 0.083 m/h) in dead-end mode. The membranes were hydraulically backwashed repeatedly at a constant interval with the pure water (hypochlorite was added to the backwash water when NOM-containing water was used), which was stored in a pressurized tank at 500 kPa. While the filter was being backwashed, the membrane feed water was transferred to an optical particle counter (ZVM, Fuji Electric Systems Co., Tokyo, Japan), which covers a particle diameter range from 0.5 to 400 μm, for measurement of the size distribution of the floc particles. Before entering the optical particle counter, the membrane feed water was diluted with 5 parts pure water to satisfy the flow rate requirement and the requirement for maximum particle number counting. The optical particle counter was calibrated with polystyrene latex particles and covered a size range from 0.5 to 400 μm. Measurements were conducted several times, and the data were averaged to give the size distribution of the floc particles for a given set of coagulation–flocculation conditions.

Two types of water were used. Water containing inorganic ions but no natural organic matter (NOM) was artificially synthesized from pure water as a model membrane feed water; the inorganic ion concentrations were adjusted equal to those of Lake Sagami water by adding reagent-grade salts (Wako Pure Chemical Industries, Osaka, Japan). The turbidity of the NOM-free water was adjusted to 0.3 mg/L with kaolin (Kanto Chemical Co., Tokyo, Japan). Water samples containing NOM were prepared from pure water, kaolin, and water from Lake Hakucho and the Chibaberi River (Hokkaido, Japan) after filtration through a membrane filter (nominal pore size, 0.45 μm). Dissolved organic carbon (DOC) and UV absorbance at a wavelength of 260 nm were quantified (DOC: Model 900, Sievers Instruments, Boulder, CO, USA; UV260: Model UV-1700, Shimadzu Co., Kyoto, Japan). PACl, S-PAC and PAC dose rates were determined after conducting some short-term preliminary experiments.

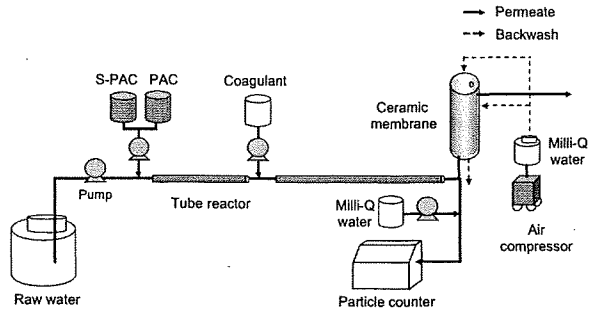

Fig. 1 – Laboratory-scale MF system.

2.3. *Activated carbon*

The S-PAC in the MF experiments was obtained by micro-grinding thermally activated, wood-based PAC (Taikou-W, Futamura Chemical Industries Co., Gifu, Japan) in a wet bead-mill. The median diameter of the as-received PAC was 7.6 μm, and about 70% by volume of the PAC particles were larger than 5 μm. Micro-grinding yielded a median diameter of 0.88 μm; the effective diameter was 0.22 μm, and 70% by volume of the S-PAC particles were smaller than 1 μm. No decant and other cleanup were conducted for the S-PAC and the PAC before use.

3. Results and discussion

3.1. *TMP buildup in pilot-scale MF experiment*

In previous studies, we found that better NOM and geosmin removal could be obtained with adsorption pretreatment using S-PAC instead of PAC in ceramic membrane MF (Matsui et al., 2005; Matsui et al., 2007), and the S-PAC dose was at least 75% less than the PAC dose. We used these results to choose the adsorbent doses for the current experiments in the three parallel lines of the pilot-scale MF system to evaluate the effects of S-PAC and PAC on membrane permeability and fouling. An S-PAC dose of 1 mg/L was used for Line 1, and a PAC dose of 5 mg/L was used for Line 2. Line 3 was operated without activated carbon as a control. First, we evaluated the effect of S-PAC pretreatment by comparing the results for Lines 1 and 3. A lower rate of TMP buildup over 63 days of operation was observed for MF after S-PAC adsorption and coagulation pretreatments than for MF after coagulation pretreatment alone (the upper panel of Fig. 2). For the first 30 days of operation, Line 3 showed only a slightly higher TMP than Line 1, and this slight difference may have been partly due to the difference in the initial permeability of the membranes. The difference in TMPs between Line 3 and Line 1 increased as the operation was extended to 63 days. Lower rates of TMP increase when MF was preceded by S-PAC adsorption pretreatment were also observed in previous studies, but for shorter operational times of 6 and 22 days (Matsui et al., 2006; Matsui et al., 2007).

The lowering of the rate of TMP increase by S-PAC was confirmed by data obtained from another experiment, in which only two parallel lines of MF were operated: Line 1 with

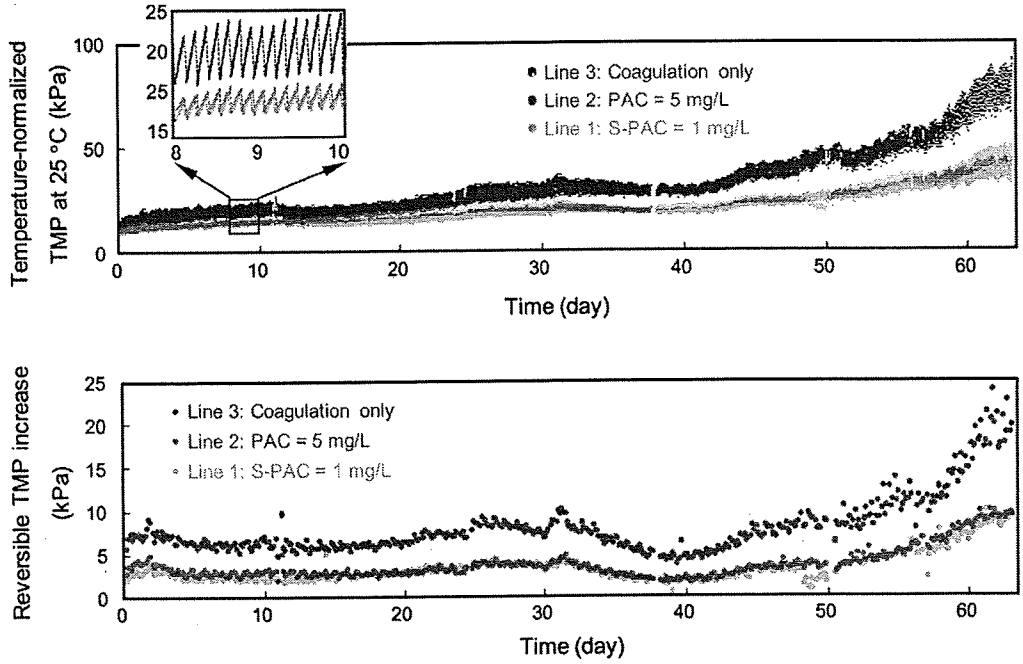

Fig. 2 – Temporal variations of TMP (upper panel) and reversible TMP increase for each batch filtration (lower panel) for Lines 1–3 of the pilot-scale MF system (PACl dose = 0.8 mg-Al/L, S-PAC/PAC contact time = 2 min, coagulation time = 2 min, $G = 200\ s^{-1}$, GT = 24,000, pH = 6.8, MF flux = 3 m/d, backwash interval = 3 h, Lake Sagami water, turbidity = 5–31 NTU, average turbidity = 10 NTU, TOC = 1.1–1.5 mg/L, average TOC = 1.2 mg/L). The small window in the upper panel shows temporal variation of TMP on days 8–10.

S-PAC and Line 3 without S-PAC. As shown in Fig. 3, during MF without S-PAC pretreatment (Line 3), the TMP tripled (from 12 to 48 kPa) over the course of 54 days. In contrast, during MF with S-PAC pretreatment (Line 1), the TMP increase was substantially less over the operation period (the TMP increased from 12 to 18 kPa). Even though the coagulant dose for Line 1 was 0.5 mg-Al/L and lower than 0.8 mg-Al/L of Line 3, which could not have been beneficial for filterability, Line 1 exhibited a lower TMP increase over the operational period. Note that membrane fouling by S-PAC was not observed. We believe that the S-PAC adsorbed membrane-fouling substances, including some of the NOM, thereby attenuating the decrease in membrane permeability during filtration.

As shown in the upper panel of Fig. 2, the adsorption pretreatment with normal PAC also lowered the TMP buildup rate. TMP buildup rates were similar for S-PAC pretreatment at 1 mg/L and PAC pretreatment at 5 mg/L. This similarity indicates that membrane-fouling substances were removed to a similar extent by S-PAC and PAC, even though the S-PAC dose was 20% of the PAC dose. As mentioned above, we previously found that similar NOM-removal efficiencies are obtained with PAC and with S-PAC at 1/4 the dose. Because NOM may have been a major membrane-fouling substance in the current system, the similar TMP buildup rates observed for the PAC (5 mg/L) and the S-PAC (1 mg/L) may have been due to similar adsorptive removal of membrane-fouling substances.

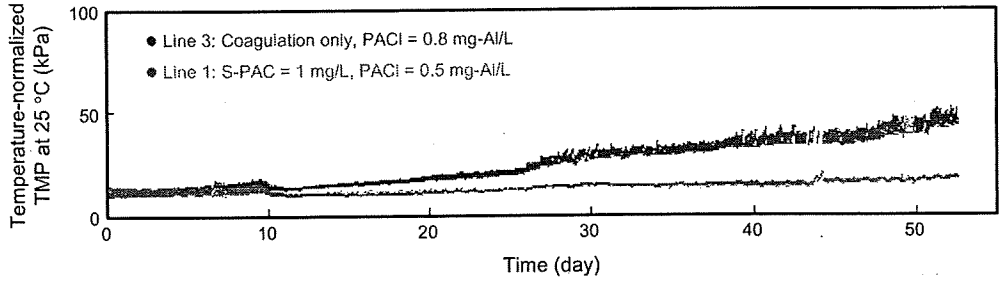

Fig. 3 – Temporal variation of TMP for Lines 1 and 3 of the pilot-scale MF system (S-PAC contact time = 2 min, coagulation time = 2 min, $G = 200\ s^{-1}$, GT = 24,000, pH = 6.8, MF flux = 3 m/d, backwash interval = 3 h, Lake Sagami water, turbidity = 6.1–69 NTU, average turbidity = 17 NTU, TOC = 0.7–1.5 mg/L, average TOC = 1.0 mg/L).

A closer look at the TMP rise over time (the small window in the upper panel of Fig. 2) revealed a saw-toothed pattern in the TMP change. The amplitudes of the TMP increases in each batch filtration were almost the same for the S-PAC and PAC pretreatments (Lines 1 and 2), but the amplitudes were larger for coagulation only (Line 3). The drops in TMP were due to periodic cleaning of the membrane by hydraulic backwashing. Although most of the TMP increase that occurred during each batch filtration was physically reversible, the hydraulic backwashing procedure did not always restore the TMP to the initial value, because the membrane fouling could not be completely cleared. Therefore, there was a long-term buildup of TMP over the 63 days of operation. The reversible TMP increase in each batch filtration was calculated by subtracting the TMP after the backwash from the corresponding TMP just before the backwash, and the increases were plotted over the entire operation period (the lower panel of Fig. 2). The amplitudes of the TMP increases due to physically reversible fouling were similar for MF with S-PAC (1 mg/L) and PAC (5 mg/L) pretreatments. The TMP increases were smaller for MF with adsorbent pretreatment (Lines 1 and 2) than without (Line 3). There are two possible explanations for this result: (1) substances that caused physically reversible fouling (such as NOM) were adsorbed by the activated carbon and (2) substances that caused physically reversible fouling were greatly modified. The latter would indicate that the floc particles formed in the presence of adsorbent were more porous than the particles that formed in the absence of adsorbent, so that the caked fouling layer built up on the membrane surface was more permeable. Although our previous results may support the first explanation (Matsui et al., 2004; Matsui et al., 2005), evidence for the second explanation will be described in the next section. Our experiments indicated that the concern that the addition of S-PAC might accelerate TMP increase is unwarranted; we showed that the addition of S-PAC efficiently attenuated both reversible and irreversible membrane fouling.

3.2. *TMP buildup in laboratory-scale MF experiment*

We also studied the effect of S-PAC pretreatment using a laboratory-scale MF setup. A particle counter was built into the setup so that the size distribution of floc particle entering the membrane could be monitored. For each batch filtration, the TMP increase caused by physically reversible membrane fouling was measured. Long-term TMP buildup caused by physically irreversible fouling was not studied, because the operation period of the laboratory-scale experiment was shorter than that of the pilot-scale experiment, owing to the limited amount of stored raw water.

1) Effect of activated carbon pretreatment on floc particle size

For a preliminary test, the size distributions of floc particles produced in the tube reactor of the laboratory-scale MF setup were measured by using the particle counter (MF was not conducted), and the effect of S-PAC and PAC addition on flocculation was studied. The flocculation experiments were conducted by changing the length of the reactor tube [and thus the mixing time and the resulting GT (the product of the velocity gradient, G, and mixing time, T) value]. The floc size increased with increasing GT value, and S-PAC enhanced flocculation for GT values larger than 19,000 (below this value, no flocculation was observed; Fig. 4). Larger floc particles were clearly formed when S-PAC was added; the floc particles were smaller for PAC and even smaller for coagulation alone. The increased flocculation rates observed with S-PAC and PAC relative to the rates for coagulation alone can be explained by the increased volume concentration of particles, according to the orthokinetic flocculation theory. This theory holds that the particle–particle collision frequency, and thereby the rate of flocculation, increases proportionally with the volume concentration of particles to be flocculated (e.g., Elimelech et al., 1998). However, we expected to observe identical flocculation rates with S-PAC and PAC, because we thought that the volume concentration of activated carbon particles in the S-PAC system would be equal to that in the PAC system from the standpoint of mass conservation. However, the flocculation rates were not the same. The addition of S-PAC enhanced flocculation more than PAC at the same dose. Aggregates adopt a fractal structure when growing, so that aggregates formed starting from small primary particles have more porous and thus a higher effective floc volume than aggregates that formed from large primary particles; the higher effective floc volume increases the collision frequency, which in turn leads to more-rapid aggregation. As consequence of

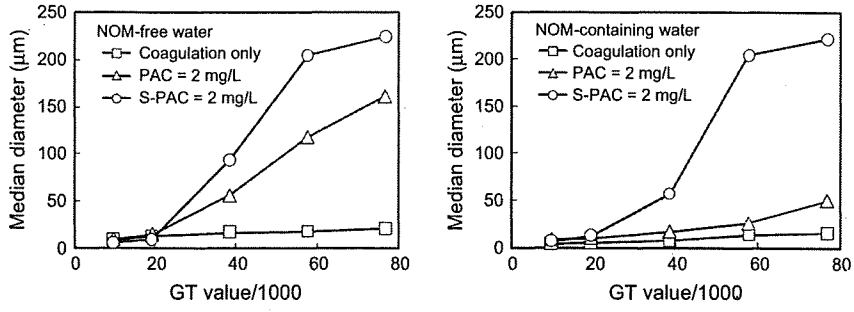

Fig. 4 – Variation of median diameter of floc particles with GT value: (left panel) NOM-free water and (right panel) NOM-containing water (PACl dose = 1 mg-Al/L, S-PAC/PAC contact time = 21 s, $G = 160\ s^{-1}$, $T = 1$–8 min, $GT = 9600$–76,800; NOM source: Lake Hakucho water, DOC = 4.6 mg/L, UV260 = 0.075 cm^{-1}).

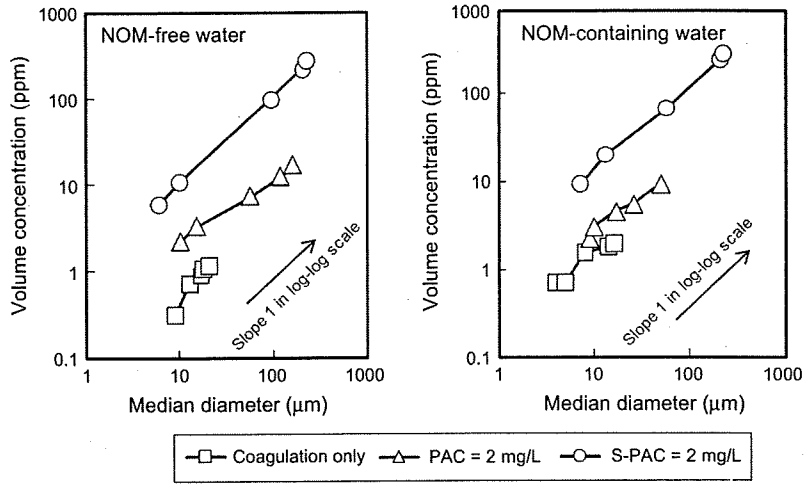

Fig. 5 – Relationship between volume concentration of total floc particles and median diameter of floc particles (left panel) NOM-free water and (right panel) NOM-containing water. (Experimental conditions are described in Fig. 4).

the fractal structure, the floc density, ρ, decreases appreciably as the particle size, d, decreases (Tambo and Watanabe, 1979; Elimelech et al., 1998):

$$\rho \propto d^{d_F-3} \quad (1)$$

where d_F is the mass fractal dimension.

The mass is kept constant during the coagulation, and the total volume fraction, ϕ, is related to the density, ρ (Oles, 1992; Serra and Casamitjana 1998):

$$\rho \propto 1/\phi \quad (2)$$

Therefore,

$$\phi \propto d^{3-d_F} \quad (3)$$

For a typical mass fractal dimension value of 2 (Tambo and Watanabe, 1979; Tambo and Francois, 1991; Elimelech et al., 1998), the total volume concentration of floc particles increases roughly in proportion with the increase of floc particle size. Fig. 5 shows the change of the total volume concentration of floc particles, which was calculated from the data obtained with the particle counter, during the course of floc growth; floc growth was quantitatively indexed by the median diameter of the floc particles. The total volume concentration increased substantially with floc growth, and the total volume concentration increased with floc size with a slope of 1 on a log–log scale, which indicates the fractal structure with a fractal dimension of 2. Moreover, the total volume concentration of floc particles was larger in the S-PAC system than in the PAC system even though the S-PAC and PAC doses were the same. This result proves that the aggregates formed starting from smaller primary particles had more porous and thus a greater effective floc volume. We concluded that this was the mechanism by which the addition of S-PAC increased the collision frequency and enhanced flocculation more than did PAC.

We also conducted flocculation experiments using NOM-containing water. Interestingly, the effect of activated carbon on flocculation was more prominent for NOM-containing water than for NOM-free water: small floc particles were formed for the GT values in the tested range in the presence of the PAC and for coagulation alone. For example, floc particles with a median diameter of 200 μm were formed with S-PAC addition at a GT value of 55,000, whereas PAC addition produced floc particles with a 25 μm median diameter at the same GT value (Fig. 4, right panel). With NOM-free water and a GT value of 57,600, the median diameter of the floc particles formed was 200 μm with S-PAC addition and 110 μm with PAC

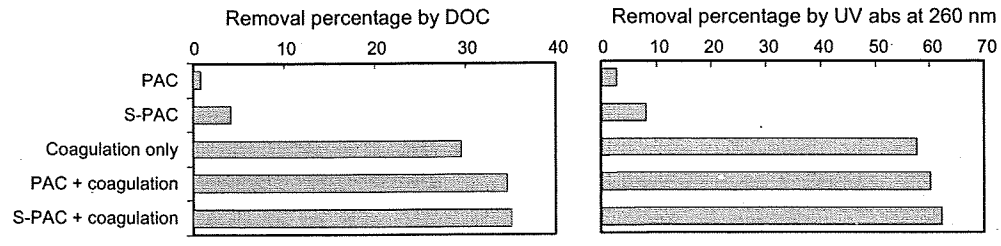

Fig. 6 – Comparison of NOM removal performances of S-PAC and PAC for the MF influent (S-PAC and PAC doses = 2 mg/L, PACl dose = 1 mg-Al/L, S-PAC/PAC contact time = 21 s, coagulation time = 4 min, G = 160 s^{-1}, GT = 38,400; NOM source: Lake Hakucho water, DOC = 4.6 mg/L, UV260 = 0.075 cm^{-1}).

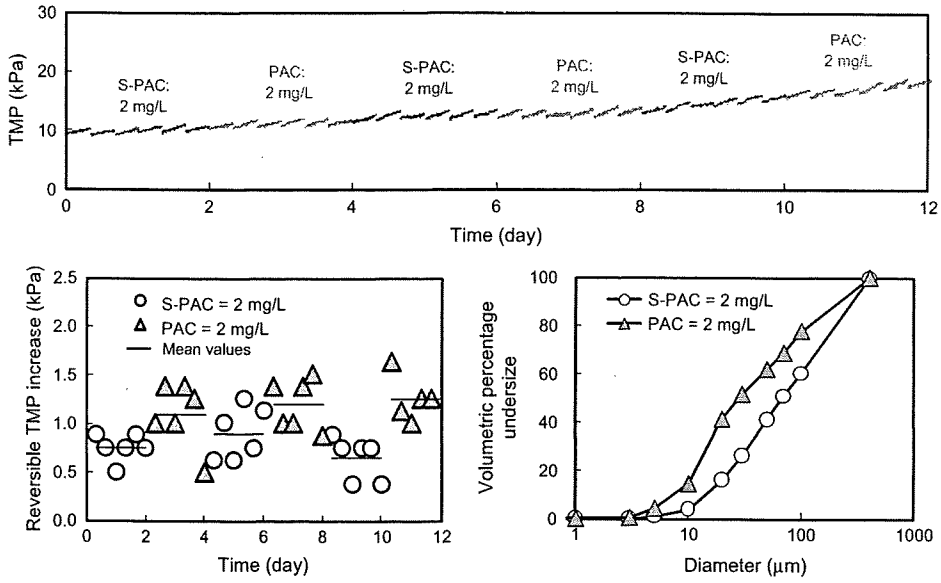

Fig. 7 – TMP (upper panel), reversible TMP increase for each batch filtration (lower left panel), and floc size distributions of MF influent (lower right panel) in the laboratory-scale MF system with alternating addition of S-PAC and PAC (S-PAC and PAC doses = 2 mg/L, PACl dose = 1 mg-Al/L, S-PAC/PAC contact time = 21 s, coagulation time = 4 min, G = 160 s^{-1}, GT = 38,400, MF flux = 0.083 m/h, backwash interval = 8 h, NOM-free water).

addition (Fig. 4, left panel). Higher NOM removal by S-PAC may have been the reason for this result. NOM (humic substances in particular) is removed by coagulation and thus consumes coagulant. Therefore, coagulation of turbidity and activated carbon particles could be hindered by the presence of NOM, but S-PAC adsorbed humic substances efficiently before the start of the coagulation reaction and enhanced coagulation. Higher NOM-removal efficiency was observed for S-PAC than for PAC, although NOM-removal efficiencies for both S-PAC and PAC were low, and the difference was not great in terms of either DOC content or UV260 value (Fig. 6). The low NOM removals can be explained by the low content of humic substances in the NOM, as indicated by the low SUVA (specific ultraviolet absorbance) value of 1.6 L/(mg m). Finally, we believe that the merit of S-PAC in terms of coagulation and flocculation arose from two effects, one chemical and one physical: enhanced coagulation by the removal of coagulant-consuming NOM and enhanced flocculation caused by increased particle–particle collision frequency, respectively.

2) Effect of floc particle size on TMP during MF

Next we conducted MF experiments to see how floc particle size affected membrane permeability during MF. First, NOM-free water was used to evaluate the effect of floc particle size in the absence of NOM as a membrane foulant. When the system was dosed with S-PAC and PAC alternately every 2 days, the TMP changed as shown in the upper panel of Fig. 7. Reversible TMP increases in each batch filtration differed for the S-PAC and PAC pretreatments (the lower left panel of Fig. 7). At the beginning of the operation, S-PAC (2 mg/L) was injected into the water, and the reversible TMP increase was 0.5–0.9 kPa. After PAC (2 mg/L) was substituted for S-PAC on day 2, the reversible TMP increase increased to 1.0–1.4 kPa. When S-PAC was substituted for PAC again on day 4, the reversible TMP increase decreased. Overall, the reversible TMP increase was smaller when the water was treated with S-PAC than when it was treated with PAC, which indicates the superiority of S-PAC for reducing physically reversible membrane fouling. The size distributions of the floc particles entering the membrane differed for the two activated carbons (the lower right panel of Fig. 7): larger floc particles were formed when the water was treated with S-PAC than when it was treated with PAC. This result indicates that the attenuation of TMP buildup was attributable to the formation of larger floc particles, which we believe would give the layer caked on the membrane surface greater porosity and greater permeability. Furthermore, according to the results shown in Fig. 5, floc particles formed in the presence of S-PAC were more porous and less compact than those formed in the presence of PAC, and this difference should have contributed to making a more permeable filter cake. The ability of S-PAC to attenuate the TMP increase was more clearly observed for the NOM-containing water, as expected from the effect on coagulation and flocculation described in the previous section. The TMP increase was reduced when S-PAC was added to the system, but a higher TMP increase was observed when PAC was added (the upper and lower left panels of Fig. 8). The floc particles that entered the membrane after S-PAC addition were much larger than those that entered the membrane after PAC addition (the lower right panel of Fig. 8).

In the pilot-scale MF experiment, S-PAC at 1 mg/L and PAC at 5 mg/L showed similar TMP increases, as described in the previous section. Given these results, we compared the changes in TMP at low S-PAC and high PAC doses (S-PAC = 0.5 mg/L and PAC = 2 mg/L) in the laboratory-scale MF

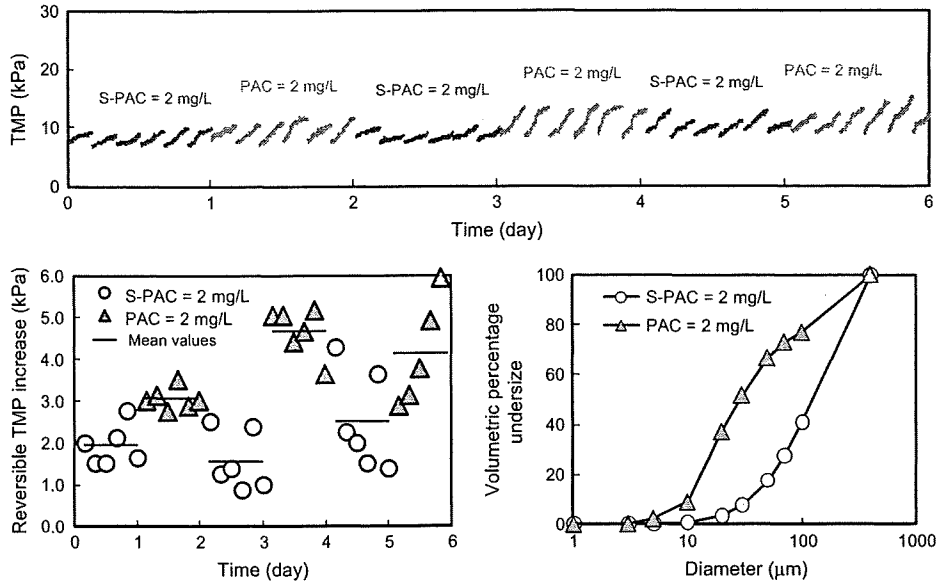

Fig. 8 – TMP (upper panel), reversible TMP increase for each batch filtration (lower left panel), and floc size distributions of MF influent (lower right panel) in the laboratory-scale MF system with alternating addition of S-PAC and PAC (S-PAC and PAC doses = 2 mg/L, PACl dose = 1.5 mg-Al/L, S-PAC/PAC contact time = 21 s, coagulation time = 4 min, $G = 160\ s^{-1}$, GT = 38,400, MF flux = 0.083 m/h, backwash interval = 4 h, NOM-containing water; NOM source: Chibaberi River water, DOC = 1.8 mg/L, UV260 = 0.06 cm^{-1}).

system. Neither the TMP increase for the entire operation period nor the reversible TMP increase for each batch filtration differed between S-PAC and PAC (the upper and lower left panels of Fig. 9). Examination of the particle-size distribution data revealed that floc particles of similar size distributions were formed with 0.5 mg/L S-PAC and 2 mg/L PAC (the lower right panel of Fig. 9). Therefore, the TMP increase in each batch filtration was highly controlled by floc particle size and probably did not greatly depend on the size of the original particles added.

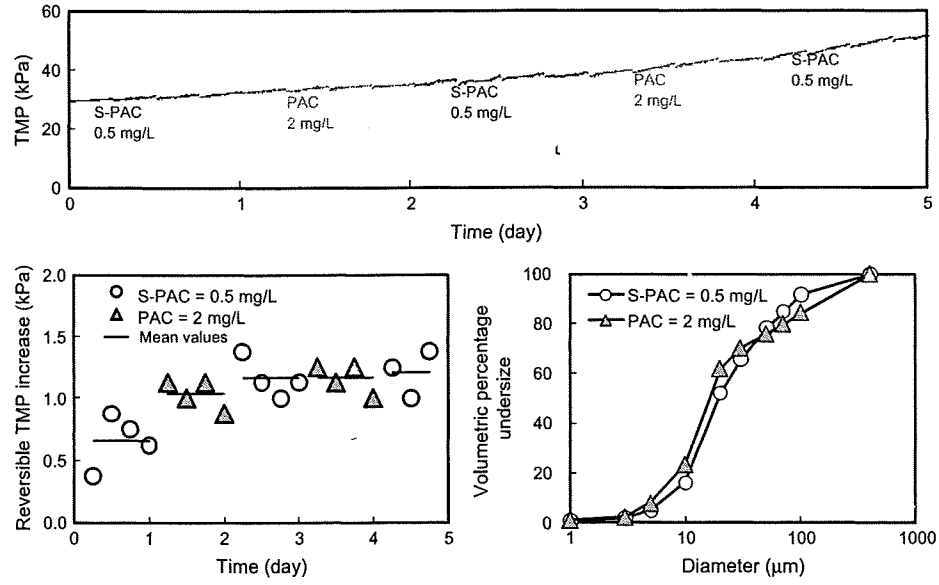

Fig. 9 – TMP (upper panel), reversible TMP increase for each batch filtration (lower left panel), and floc size distributions of MF influent (lower right panel) in the laboratory-scale MF system at a reduced adsorbent dose of S-PAC and a full dose of PAC (PACl dose = 1 mg-Al/L, S-PAC/PAC contact time = 21 s, coagulation time = 4 min, $G = 160\ s^{-1}$, GT = 38,400, MF flux = 0.083 m/h, backwash interval = 6 h, NOM-free water).

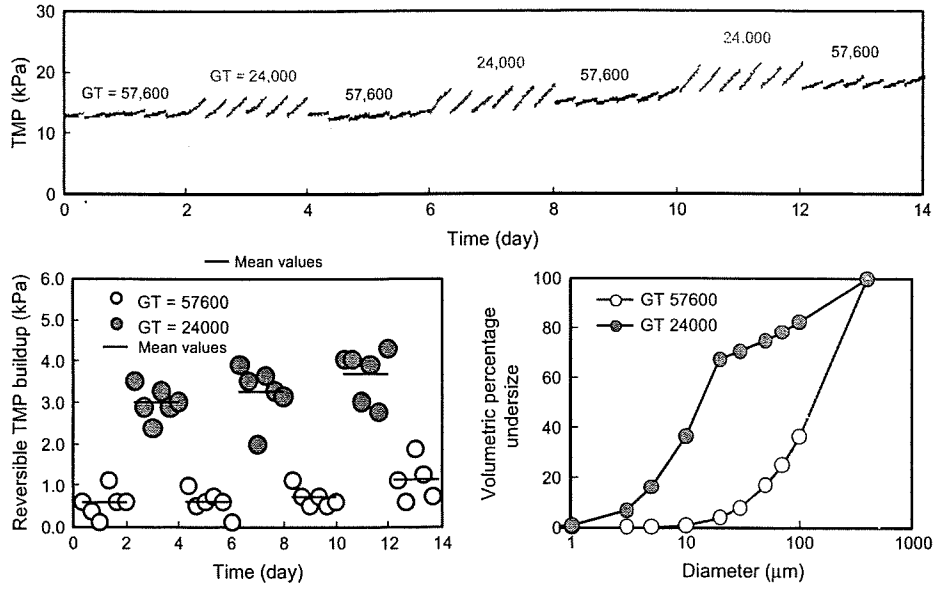

Fig. 10 – TMP (upper panel), reversible TMP increase for each batch filtration (lower left panel), and floc size distributions of MF influent (lower right panel) in the laboratory-scale MF system at different GT values (S-PAC dose = 2 mg/L, PACl dose = 1 mg-Al/L, S-PAC/PAC contact time = 21 s, GT = 24,000 = 320 s^{-1} × 1 min + 160 s^{-1} × 30 s or GT = 57,600 = 320 s^{-1} × 1 min + 160 s^{-1} × 4 min, MF flux = 0.083 m/h, backwash interval = 8 h, NOM-free water).

The volume concentrations of floc particles were 3.8 ppm for S-PAC at 0.5 mg/L and 2.0 ppm for PAC at 2.0 mg/L (data not shown). That is, the volume concentration of floc particles was higher for S-PAC at 0.5 mg/L than for PAC at 2.0 mg/L, although the mass concentration was lower. This result clearly shows that the floc particles formed after the addition of S-PAC had higher porosity and thus should have had higher permeability as they built up on the membrane surface. We next examined the effect of floc particle size on the TMP buildup rate with different flocculation times by changing the length of the reactor tube (and the resulting GT value), which produced different sizes of floc particles. Two flow lines with different detention times for coagulation and flocculation were setup and used alternately every 2 days in an experiment. One flow line had a GT value of 24,000, and the other had a GT value of 57,600. The membrane filtration experiment started with the high GT value (57,600). At this GT value, the reversible TMP increase for each batch filtration was less than 0.1 kPa (the upper and lower left panels of Fig. 10). After 2 days of operation, the coagulation–flocculation condition was changed to the low GT value (24,000), and higher rates of TMP buildup (about 3 kPa) were observed. The TMP buildup declined when the GT value was increased again. This GT-value-related change in the TMP buildup rate was repeated every time the GT value was changed. The median size of floc particles formed at GT = 57,600 was 160 μm, whereas it was 15 μm at GT = 24,000 (the lower right panel of Fig. 10). These data clearly show that the size of floc particles entering the membrane affected the reversible TMP increase and the permeability of the cake-layer formed on the membrane. In this paper, the effects of S-PAC pretreatment on coagulation and TMP buildup during microfiltration were discussed mainly by focusing on floc particle size. Coagulation, however, is basically complex phenomena, which is better understood by floc particle size and other characteristics. More studies are still needed.

4. Conclusions

1) The addition of S-PAC did not reduce membrane permeability. Instead, the S-PAC attenuated the long-term (63 days) TMP buildup that could not be reversed by hydraulic backwashing. The addition of PAC also attenuated the long-term TMP buildup, but at a dose that was 5 times the S-PAC dose. The better TMP attenuation ability of S-PAC may have been due to the fact that S-PAC removed NOM more efficiently than PAC or coagulation alone.
2) Because the addition of S-PAC or PAC resulted in the formation of larger floc particles, the reversible TMP increase during each filtration cycle was mitigated by pretreatment with S-PAC or PAC.
3) Addition of S-PAC depressed reversible TMP increases more effectively than did addition of PAC because larger, more permeable floc particles were formed with S-PAC than with PAC at the same dose. Larger, more permeable floc particles were formed with S-PAC because of the increased volume concentration due to the fractal effect and the increased frequency of particle–particle collisions.
4) Another reason for the difference in floc particle size may have been differences in the degree to which NOM hindered coagulation: more NOM may have been adsorbed by S-PAC than by PAC and by coagulation alone. As a result, more of the coagulant may have been available for effective coagulation.

Acknowledgements

This study was supported by a Grant-in-Aid for Scientific Research B and A (no. 19360235 and 21246083) from the Ministry of Education, Science, Sports and Culture of the Government of Japan, by a research grant from the Ministry of Health, Labor and Welfare, and by Metawater Co., Tokyo, Japan. The pilot-scale MF experiments were conducted as a study of the e-Water Project II of the Japan Water Research Center at Kawai Water Purification Plant of the Waterworks Bureau, Yokohama, Japan.

REFERENCES

Adham, S.S., Snoeyink, V.L., Clark, M.M., Bersillon, J.L., 1991. Predicting and verifying organics removal by PAC in an ultrafiltration system. J. Am. Water Works Assoc. 83 (12), 81–91.

Barbot, E., Moustier, S., Bottero, J.Y., Moulin, P., 2008. Coagulation and ultrafiltration: understanding of the key parameters of the hybrid process. J. Membr. Sci. 325, 520–527.

Baudin, I., Campos, C., Laîné, J.M., 2001. Removal of organic matter by the PAC-UF process: first two years of a full-scale application. Water Sci. Technol.: Water Supply 1 (4), 253–263.

Carroll, T., King, S., Gray, S.R., Bolto, B.A., Booker, N.A., 2000. The fouling of microfiltration membranes by NOM after coagulation treatment. Water Res. 34 (11), 2861–2868.

Chen, Y., Dong, B.Z., Gao, N.Y., Fan, J.C., 2007. Effect of coagulation pretreatment on fouling of an ultrafiltration membrane. Desalination 204, 181–188.

Cho, M.-H., Lee, C.-H., Lee, S., 2005. Influence of floc structure on membrane permeability in the coagulation-MF process. Water Sci. Technol. 51 (6–7), 143–150.

Choi, K.Y.-j., Dempsey, B.A., 2004. In-line coagulation with low-pressure membrane filtration. Water Res. 38 (19), 4271–4281.

Elimelech, M., Williams, R., Gregory, J., Jia, X., 1998. Particle Deposition and Aggregation. Butterworth-Heinemann.

Fan, L., Nguyen, T., Roddick, F.A., Harris, J.L., 2008. Low-pressure membrane filtration of secondary effluent in water reuse: pre-treatment for fouling reduction. J. Membr. Sci. 320, 135–142.

Gray, S.R., Ritchie, C.B., Tran, T., Bolto, B.A., Greenwood, P., Busetti, F., Allpike, B., 2008. Effect of membrane character and solution chemistry on microfiltration performance. Water Res. 42 (3), 743–753.

Haberkamp, J., Ruhl, A.S., Ernst, M., Jekel, M., 2007. Impact of coagulation and adsorption on DOC fractions of secondary effluent and resulting fouling behavior in ultrafiltration. Water Res. 41 (17), 3794–3802.

Howe, K.J., Marwah, A., Chiu, K.-P., Adham, S.S., 2006. Effect of coagulation on the size of MF and UF membrane foulants. Environ. Sci. Technol. 40 (24), 7908–7913.

Huang, H., Schwab, K., Jacangelo, J.G., 2009. Pretreatment for low pressure membranes in water treatment: a review. Environ. Sci. Technol. 43 (9), 3011–3019.

Jack, A.M., Clark, M.M., 1998. Using PAC-UF to treat a low-quality surface water. J. Am. Water Works Assoc. 90 (11), 83–95.

Jang, H.-N., Lee, D.-S., Park, M.-K., Moon, S.-Y., Cho, S.-Y., Kim, C.-H., Kim, H.-S., 2006. Effects of the filtration flux and pre-treatments on the performance of a microfiltration drinking water treatment system. Water Sci. Technol.: Water Supply 6 (4), 81–87.

Judd, S.J., Hillis, P., 2001. Optimization of combined coagulation and microfiltration for water treatment. Water Res. 35 (12), 2895–2904.

Kanaya, S., Fujiura, S., Tomita, Y., Yonekawa, H., 2007. The world's largest ceramic membrane drinking water treatment plant. In: Proc. AWWA Membrane Technol. Conf., Tampa, FL, USA.

Kimura, K., Maeda, T., Yamamura, H., Watanabe, Y., 2008. Irreversible membrane fouling in microfiltration membranes filtering coagulated surface water. J. Membr. Sci. 320, 356–362.

Lahoussine-Turcaud, V., Wiesner, M.R., Bottero, J.-Y., Mallevaille, J., 1990. Coagulation pretreatment for ultrafiltration of a surface water. J. Am. Water Works Assoc. 82 (12), 76–81.

Laîné, J.-M., Hagstrom, J.P., Clark, M.M., Mallevialle, J., 1989. Effects of ultrafiltration membrane composition. J. Am. Water Works Assoc. 81 (11), 61–67.

Lee, J.D., Lee, S.A., Jo, M.H., Park, P.K., Lee, C.H., Kwak, J.W., 2000. Effect of coagulation conditions on membrane filtration characteristics in coagulation–microfiltration process for water treatment. Environ. Sci. Technol. 34 (17), 3780–3788.

Lee, S.A., Fane, A.G., Waite, T.D., 2005. Impact of natural organic matter on floc size and structure effects in membrane filtration. Environ. Sci. Technol. 39 (17), 6477–6486.

Leiknes, T., Odegaard, H., Myklebust, H., 2004. Removal of natural organic matter (NOM) in drinking water treatment by coagulation–microfiltration using metal membranes. J. Membr. Sci. 242 (1–2), 47–55.

Li, C.-W., Chen, Y.-S., 2004. Fouling of UF membrane by humic substance: effects of molecular weight and powder-activated carbon (PAC) pre-treatment. Desalination 170, 59–67.

Loi-Brügger, A., Panglisch, S., Buchta, P., Hattori, K., Yonekawa, H., Tomita, Y., Gimbel, R., 2006. Ceramic membranes for direct river water treatment applying coagulation and microfiltration. Water Sci. Technol.: Water Supply 6 (4), 89–98.

Mallevialle, J., 1996. Water Treatment Membrane Processes. McGraw-Hill, New York, NY, USA.

Matsui, Y., Fukuda, Y., Murase, R., Aoki, N., Mima, S., Inoue, T., Matsushita, T., 2004. Micro-ground powdered activated carbon for effective removal of natural organic matter during water treatment. Water Sci. Technol.: Water Supply 4 (4), 155–163.

Matsui, Y., Murase, R., Sanogawa, T., Aoki, N., Mima, S., Inoue, T., Matsushita, T., 2005. Rapid adsorption pretreatment with submicron powdered activated carbon particles before microfiltration. Water Sci. Technol. 51 (6–7), 249–256.

Matsui, Y., Sanogawa, T., Aoki, N., Mima, S., Matsushita, T., 2006. Evaluating submicron-sized activated carbon adsorption for microfiltration pretreatment. Water Sci. Technol.: Water Supply 6 (1), 149–155.

Matsui, Y., Aizawa, T., Kanda, F., Nigorikawa, N., Mima, S., Kawase, Y., 2007. Adsorptive removal of geosmin by ceramic membrane filtration with super-powdered activated carbon. J. Water Supply Res. Technol. AQUA 56 (6–7), 411–418.

Matsui, Y., Ando, N., Sasaki, H., Matsushita, T., Ohno, K., 2009. Branched pore kinetic model analysis of geosmin adsorption on super-powdered activated carbon. Water Res. 43 (12), 3095–3103.

Mozia, S., Tomaszewska, M., Morawski, A.W., 2005. Studies on the effect of humic acids and phenol on adsorption–ultrafiltration process performance. Water Res. 39 (2–3), 501–509.

Oh, J.-I., Lee, S.H., 2005. Influence of streaming potential on flux decline of microfiltration with inline rapid pre-coagulation process for drinking water production. J. Membr. Sci. 254, 39–47.

Oles, V., 1992. Shear-induced aggregation and breakup of polystyrene latex particles. J. Colloid Interface Sci. 154 (2), 351–358.

Park, P.-k., Lee, C.-h., Choi, S.-J., Choo, K.-H., Kim, S.-H., Yoon, C.-H., 2002. Effect of the removal of DOMs on the performance of a coagulation-UF membrane system for drinking water production. Desalination 145, 237–245.

Park, P.K., Lee, C.H., Lee, S., 2006. Variation of specific cake resistance according to size and fractal dimension of chemical

flocs in a coagulation–microfiltration process. Desalination 199, 213–215.
Park, P.K., Lee, C.H., Lee, S., 2007. Determination of cake porosity using image analysis in a coagulation–microfiltration system. J. Membr. Sci. 293, 66–72.
Pikkarainen, A.T., Judd, S.J., Jokela, J., Gillberg, L., 2004. Pre-coagulation for microfiltration of an upland surface water. Water Res. 38 (2), 455–465.
Serra, T., Casamitjana, X., 1998. Structure of the aggregates during the process of aggregation and breakup under a shear flow. J. Colloid Interface Sci. 206 (2), 505–511.
Takizawa, S., Zhao, P., Ohgaki, S., Katayama, H., 2008. Kinetic analysis of PAC cake-layer formation in hybrid PAC-MF systems. Water Sci. Technol.: Water Supply 8 (1), 1–7.
Tambo, N., Watanabe, Y., 1979. Physical characteristics of flocs I, the floc density function and aluminium floc. Water Res. 13, 409–419.
Tambo, N., Francois, R.J., 1991. Mixing, breakup, and aggregate characteristics. In: Amirtharajah, A., Clark, M.M., Trussell, R.R. (Eds.), Mixing in Coagulation and Flocculation. Am. Water Works Assoc.
Tomaszewska, M., Mozia, S., 2002. Removal of organic matter from water by PAC/UF system. Water Res. 36 (16), 4137–4143.
Yiantsios, S.G., Karabelas, A.J., 2001. An experimental study of humid acid and powdered activated carbon deposition on UF membranes and their removal by backwashing. Desalination 140, 195–209.
Yonekawa, H., Tomita, Y., Watanabe, Y., 2004. Behavior of micro-particles in monolith ceramic membrane filtration with pre-coagulation. Water Sci. Technol. 50 (12), 317–325.
Zhang, M., Li, C., Benjamin, M.M., Chang, Y., 2003. Fouling and natural organic matter removal in adsorbent/membrane systems for drinking water treatment. Environ. Sci. Technol 37, 1663–1669.

WATER RESEARCH 43 (2009) 3095–3103

Available at www.sciencedirect.com

ScienceDirect

journal homepage: www.elsevier.com/locate/watres

Branched pore kinetic model analysis of geosmin adsorption on super-powdered activated carbon

Yoshihiko Matsui, Naoya Ando, Hiroshi Sasaki, Taku Matsushita, Koichi Ohno*

Graduate School of Engineering, Hokkaido University, N13W8, Sapporo 060-8628, Japan

ARTICLE INFO

Article history:
Received 8 December 2008
Received in revised form
2 April 2009
Accepted 9 April 2009
Published online 19 April 2009

Keywords:
PAC
Particle size
Submicron
HSDM
Taste and odor

ABSTRACT

Super-powdered activated carbon (S-PAC) is activated carbon of much finer particle size than powdered activated carbon (PAC). Geosmin is a naturally occurring taste and odor compound that impairs aesthetic quality in drinking water. Experiments on geosmin adsorption on S-PAC and PAC were conducted, and the results using adsorption kinetic models were analyzed. PAC pulverization, which produced the S-PAC, did not change geosmin adsorption capacity, and geosmin adsorption capacities did not differ between S-PAC and PAC. Geosmin adsorption kinetics, however, were much higher on S-PAC than on PAC. A solution to the branched pore kinetic model (BPKM) was developed, and experimental adsorption kinetic data were analyzed by BPKM and by a homogeneous surface diffusion model (HSDM). The HSDM describing the adsorption behavior of geosmin required different surface diffusivity values for S-PAC and PAC, which indicated a decrease in surface diffusivity apparently associated with activated carbon particle size. The BPKM, consisting of macropore diffusion followed by mass transfer from macropore to micropore, successfully described the batch adsorption kinetics on S-PAC and PAC with the same set of model parameter values, including surface diffusivity. The BPKM simulation clearly showed geosmin removal was improved as activated carbon particle size decreased. The simulation also implied that the rate-determining step in overall mass transfer shifted from intraparticle radial diffusion in macropores to local mass transfer from macropore to micropore. Sensitivity analysis showed that adsorptive removal of geosmin improved with decrease in activated carbon particle size down to 1 μm, but further particle size reduction produced little improvement.

© 2009 Elsevier Ltd. All rights reserved.

1. Introduction

An important aesthetic component of consumer satisfaction and confidence in the production and supply of drinking water is the absence of objectionable taste and odor. Objectionable taste and odor can occur naturally in source water, and unintentionally in the treatment plant and distribution system. Geosmin and 2-methylisoborneol (MIB) are probably the most common naturally occurring taste and odor compounds found and studied in water supplies. Both are metabolites of actinomycetes and some species of cyanobacteria, and are responsible for earthy, musty smelling drinking water. They impair aesthetic quality even at concentration levels of 10 ng/L or less (McGuire et al., 1981; Mallevialle and Suffet, 1987). Under Japanese water quality regulations, the concentration of geosmin and MIB in municipal drinking water supplies must be less than 10 ng/L.

* Corresponding author. Tel./fax: +81 11 706 7280.
E-mail address: matsui@eng.hokudai.ac.jp (Y. Matsui).
0043-1354/$ – see front matter © 2009 Elsevier Ltd. All rights reserved.
doi:10.1016/j.watres.2009.04.014

Nomenclature

$c_l(t, R)$	liquid phase concentration on the outer surface of an adsorbent particle (ng/L)
$C(t)$	adsorbate concentration in bulk water phase as a function of time, t (ng/L)
C_C	adsorbent concentration in bulk water (g/L)
D_S	surface diffusion coefficient (cm^2/s)
$f(R)$	normalized particle size distribution function of adsorbent (cm^{-1})
k_B	rate coefficient for mass transfer between macropore and micropore (s^{-1})
k_f	liquid film mass transfer coefficient (cm/s)
K_F	Freundlich constant $(ng/g)/(ng/L)^{1/n_F}$
n_F	Freundlich exponent (dimensionless)
$q_{AV}(t, R)$	the amount adsorbed in the solid phase per mass of adsorbent as a function of t and R(ng/g)
$q_B(t, r, R)$	solid phase concentration in micropore of an adsorbent having radius R, at radial distance r, and time t (ng/g)
$q_M(t, r, R)$	solid phase concentration in macropore of an adsorbent having radius R, at radial distance r, and time t (ng/g)
r	radial distance from the center of a PAC particle (cm)
R	adsorbent particle radius (cm)
t	time (s)
ϕ	fraction of adsorptive capacity available in macropore region (dimensionless)
ρ	adsorbent particle density (g/L)

The PAC adsorption process is the simplest and most commonly used process for removing these compounds from water, and it removes them effectively. There is a need to further improve removal efficiency, however, because the carbon usage rate is still low. A PAC dosage of 5–50 mg/L is usually required for raw water having geosmin or MIB levels of 10–100 ng/L (Lalezary-Craig et al., 1988; Cook et al., 2001): milligrams of adsorbent are required to treat nanograms of adsorbates. This is thought to result from the low adsorption capacity of geosmin and MIB in natural water, but also due to slow adsorption rates. Adsorption of geosmin and MIB is, in particular, lowered in natural water by the competitive effects with NOM (Newcombe et al., 1997; Graham et al., 2000).

Adsorption rate improves with smaller adsorbent particle size because of shorter travel distance for intraparticle radial diffusion and larger specific surface area per adsorbent mass (Sontheimer et al., 1988). However, the quantitative effect of adsorbent particle size on removal efficiency has not been researched sufficiently. Najm et al. (1990) re-emphasized the benefit of smaller PAC particle size. Traegner et al. (1996) modeled PAC adsorption in a completely stirred reactor tank at steady state and discussed the effect of adsorbent particle size and its distribution. Regrettably, these studies ignored the internal diffusivity dependency in activated carbon on adsorbent particle size. Internal diffusivity apparently decreases as the activated carbon particle size decreases; therefore the improvement of overall adsorption rate with smaller PAC particles might be reduced to some extent because of lower internal diffusion rate, although the travel distance for intraparticle radial diffusion become shorter in PAC of smaller particle size which contributes improving adsorption rate.

The phenomena of the internal diffusivity dependency on adsorbent particle size can be explained by particle pore structure and by the adsorbate transport process on the pore (Sontheimer et al., 1988). Intraparticle mass transfer resistance results partly from the local mass transfer from larger-size pores to smaller-size pores, rather than from the radial mass transfer from the outer surface to the center of an adsorbent particle. Therefore, particle size reduction by pulverization does not necessarily lead to the reduction of travel distance of mass transfer in an adsorbent particle. Accordingly, the internal diffusivity, which is assumed to be constant in homogeneous surface diffusion models (HSDM), must be recognized as apparently particle size dependent. This rather strongly implies that a two-domain model, where a spherical particle of a porous adsorbent is comprised of uniformly distributed micropores, which branch off macropores undergoing radial mass transport, would be more appropriate than HSDM (Buchholz and Krückels, 1976; Weber and Liang, 1983).

The two-domain model incorporates dual particle-diffusion: relatively rapid radial diffusion onto and adsorbing in macropore regions in the adsorbent, followed by slow diffusion from macropore to micropore and adsorbing in micropore regions. The branched pore kinetic model (BPKM) presented by Peel and Benedek (1980a,b) is a simplified version of the two-domain model. The BPKM incorporates two internal mass transfer resistances, but the micropore diffusion process is expressed by a linear driving force model. The BPKM has three parameters for describing the entire internal diffusion process instead of one parameter (surface diffusion coefficient, D_S) of HSDM, and has a strong ability to describe the adsorption process in batch reactors, where there is an initial high rate phase, followed by a lower-rate approach to equilibrium. Such behavior is consistent with the two-domain or three-domain structure of activated carbon (bi-modal and tri-modal distribution of pore size) and can be attributed to a high rate of solute movement through macropores, followed by much slower passage through micro pores (Sontheimer et al., 1988). The BPKM has recently been widely applied (Yang and Al-Duri, 2001; Ko et al., 2002, 2003, 2005; Chang et al., 2004; Ahn et al., 2005; Lua and Jia, 2007; Jia and Lua, 2008).

Super-powdered activated carbon (S-PAC) is activated carbon finer than conventional PAC. S-PAC can be produced by pulverizating PAC. Higher removal efficiency of geosmin has been attained with S-PAC dosed as a pretreatment agent for ceramic membrane microfiltration (Matsui et al., 2007). However, the mechanism of S-PAC adsorption and the adsorption rate dependency on carbon particle size, in particular the adsorption rate dependency for activated carbon with particle sizes ranging from a few micrometers down to submicrometer sizes, has not yet been analyzed.

This paper presents a theoretical analysis of the adsorption kinetics of geosmin on S-PAC and PAC. The BPKM, modified to include the adsorbent particle size distribution, is developed and a simple numerical solution method for the model is applied. The geosmin concentration decays in a batch adsorption process are fitted to the model, and the effects of adsorbent particle size and size distribution on geosmin removal at given contact times are analyzed to determine optimum adsorbent particle size.

2. Mathematical development

In developing the adsorption model, the size distribution of adsorbent particles were taken into consideration because the effect of particle size distribution, as well as average particle size itself, were to be analyzed. When considering adsorbent particle size distribution, the overall mass conservation equation of the adsorbate in a batch adsorption system is as follows:

$$\frac{dC(t)}{dt} = -C_C \int_0^\infty f(R) \frac{dq_{AV}(t, R)}{dt} dR \quad (1)$$

In BPKM, a fraction, ϕ, of total adsorption capacity belongs to macropores while the remaining fraction, $1-\phi$, belongs to micropores. Micropores are assumed to be homogeneously distributed throughout the particle and to branch off the larger macropore network, as shown in Fig. 1. Here, the macropore and micropore do not necessarily correspond to those defined by International Union of Pure and Applied Chemistry (IUPAC), in which a macropore has radius >25 nm and a micropore has radius <1 nm. In BPKM, macropore and micropore mean relatively large-size and small-size pore, respectively. The amount adsorbed in the solid phase, $q_{AV}(t, R)$, is given as the volume averaged solid phase concentration:

$$q_{AV}(t, R) = \frac{3}{R^3} \int_0^R [\phi q_M(t, r, R) + (1-\phi) \times q_B(t, r, R)] r^2 dr \quad (2)$$

The BPKM (Peel and Benedek, 1980b) describes the mass transfer mechanism in adsorption by three processes in series: (i) the external mass transfer across the liquid film surrounding the carbon particle; (ii) the radial intraparticle diffusion through macropores in an adsorbed state; and (iii) local diffusion from macropore to micropore. The surface diffusion mechanism was used to describe diffusion through the macropore region, while transfer from macropore to micropore is described by a linear driving force model.

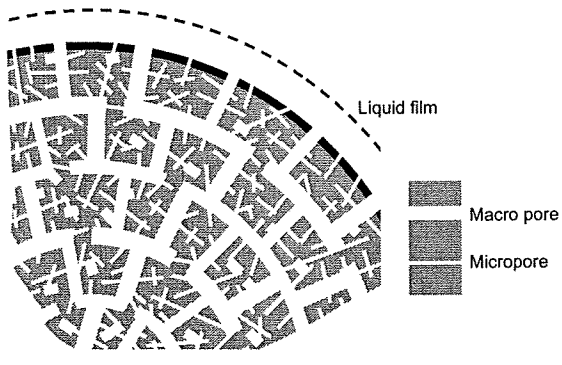

Fig. 1 – Idealized structure of activated carbon pore in BPKM.

Radial mass transport in an adsorbent particle occurs along the macropore walls by surface diffusion. The macropore mass balance equation is as follows:

$$\phi \frac{\partial q_M(t, r, R)}{\partial t} = \frac{\phi}{r^2} \frac{\partial}{\partial r} \left\{ D_S r^2 \left[\frac{\partial q_M(t, r, R)}{\partial r} \right] \right\} - k_B [q_M(t, r, R) - q_B(t, r, R)] \quad (3)$$

The mass transfer from macropore to micropore is described by linear driving force model based on the concentration difference. The micropore mass balance equation is as follows:

$$(1-\phi) \frac{\partial q_B(t, r, R)}{\partial t} = k_B [q_M(t, r, R) - q_B(t, r, R)] \quad (4)$$

In previous models (Peel and Benedek, 1980a; Ko et al., 2003, 2005), the external film balance was achieved by equating the flux at the external solid–liquid interface and the flux at the liquid film:

$$\phi D_S \frac{\partial q_M(t, r, R)}{\partial r}\bigg|_{r=R} = \frac{k_F}{\rho} [C(t) - c_l(t, R)] \quad (5)$$

In this study, however, foreseeing the application of orthogonal collocation method in the numerical solution, the external film balance is, instead of Eq. (5), described by equating mass balance and mass transfer from the external particle surface to inside the particle:

$$\frac{d}{dt} \left\{ \int_0^R [\phi q_M(t, r, R) + (1-\phi) \times q_B(t, r, R)] r^2 dr \right\} \frac{1}{R^2} = \frac{k_F}{\rho} [C(t) - c_l(t, R)] \quad (6)$$

The mass balance equation for an adsorbate in a batch container is given as follows:

$$\frac{dC(t)}{dt} = -\frac{3C_C k_F}{\rho} \int_0^\infty \frac{f(R)}{R} [C(t) - c_l(t, R)] dR \quad (7)$$

Local adsorption equilibrium is assumed on the exterior particle surface of an adsorbent particle, and the equilibrium is expressed by the Freundlich isotherm equation:

$$c_l(t, R) = \left[\frac{q_M(t, R, R)}{K_F} \right]^{n_F} \quad (8)$$

The HSDM can be yielded when the parameter ϕ is equal to one and the coefficient k_B is zero in the set of Eqs. (3)–(7).

The set of the model Eqs. (3),(4),(6),(7) and(8) for adsorption in a batch reactor was converted into a set of ordinary differential equations with respect to time t using the method of orthogonal collocation. The resultant equations were solved as a system of ordinary differential equations by the Gear's stiff method in the IMSL® Math Library, after deriving the analytical Jacobian of the equations. Details are presented in the Appendix A.

3. Materials and methods

3.1. Adsorbents

To prepare the S-PAC used in our experiments, thermally activated wood-based PAC (Taikou-W, Futamura Chemical Industries Co., Gifu, Japan) were ground in a wet bead mill (Metawater Co., Ltd., Tokyo, Japan). Both the S-PAC and the as-received (i.e., normal) PAC were used to determine the effects of particle size on adsorption effectiveness. The PAC was dried in an oven at 105 °C and stored in a desiccator. A PAC suspension was prepared and placed under vacuum to remove any air from the activated carbon pores. The S-PAC was stored in a slurry (5%) with pure water at 4 °C and used after dilution and vacuum conditioning. Particle size distributions of S-PAC and PAC were determined using laser-light scattering instruments (LMS-30 from Seishin Enterprise Co., Ltd., and Microtrac HRA from Nikkiso Co., Ltd., Tokyo, Japan).

3.2. Water samples

Geosmin solutions were prepared by diluting geosmin-MeOH liquid (Supelco, Sigma Aldrich Japan, Tokyo) with pure water (Milli-Q Advantage, Millipore Corp., Billerica, MA, USA). The solutions were diluted to a concentration of 100 ng/L with the pure water before use. Geosmin concentrations were analyzed using thermal desorption system (TDS) gas chromatography/mass spectrometry (GC/MS) and the stir bar sorptive extraction (SBSE) method (GERSTEL K.K, Tokyo, Japan, and Agilent Technologies Japan, Tokyo), using deuterium-labeled geosmin (Hayashi Pure Chemical Ind., Ltd., Osaka, Japan) as an internal standard.

3.3. Batch adsorption tests

The adsorption kinetics was investigated by means of batch tests with efficient mixing. Sample water (3 L) containing geosmin (100 ng/L) was placed in a beaker, and an aliquot was withdrawn from the beaker to determine the initial geosmin concentration. After the addition of a specified amount of activated carbon suspension, aliquots were withdrawn at intervals and filtered immediately through a 0.2 μm membrane filter (DISMIC-25HP, Toyo Roshi Kaisha, Ltd., Tokyo) for analysis of the geosmin concentration.

Aliquots (100 or 150 mL) from the 3 L solution containing geosmin and PAC were transferred to 125 or 160 -mL vials, and the vials were agitated on a shaker for 1 week. After the water samples were filtered through a 0.2 μm membrane filter, the water phase geosmin concentrations were measured by TDS-GC/MS and SBSE. The solid phase geosmin concentrations were calculated from the mass balance, and were plotted against water phase concentrations to obtain isotherm data.

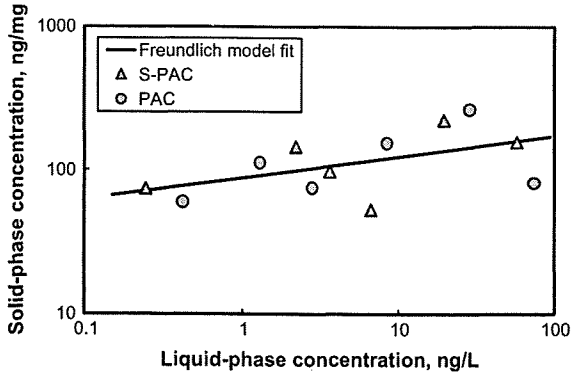

Fig. 2 – Geosmin adsorption isotherms of S-PAC and PAC were treated as one set of data and were modeled by one Freundlich equation.

4. Results and discussion

4.1. Empirical adsorption capacity and kinetics

Batch adsorption isotherm tests were conducted, and adsorption capacities on S-PAC and PAC were experimentally measured. Although the data from the isotherm experiments are scattered, they show no difference in adsorption capacity between S-PAC and PAC (Fig. 2): pulverization did not change the geosmin adsorption capacity. Pulverization did, however, increase the adsorption capacity of natural organic matter and a model substance, polystyrene sulfonate of molecular weight 1800 Da (Matsui et al., 2004), although further research is needed to confirm this phenomena of the adsorption capacity increase. We believe that activated carbon particle size reduction does not change adsorption capacity for small molecules but does for macromolecules. A higher geosmin capacity on S-PAC than on PAC was reported in a previous publication (Matsui et al., 2008), but we now speculate that it was only an artifact and due to slight heterogeneity of the PAC samples we used. Experimental data showing no difference in geosmin adsorption capacity between S-PAC and PAC were obtained when S-PAC and PAC were more carefully prepared: PAC samples for this study were first well mixed, then divided to produce sample pairs; one of the pair was used as the PAC and the other was pulverized to S-PAC.

Adsorption kinetic data clearly show faster geosmin uptake rates on S-PAC than on PAC (Fig. 3). About 90% geosmin

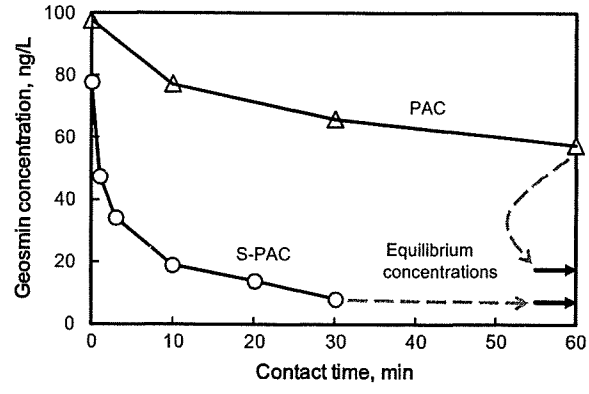

Fig. 3 – Geosmin concentration decays in batch adsorptions. Arrows in the right bottom show equilibrium concentrations attained by S-PAC and PAC, as predicted by isotherm calculations with the Freundlich equation, using the Fig. 2 data.

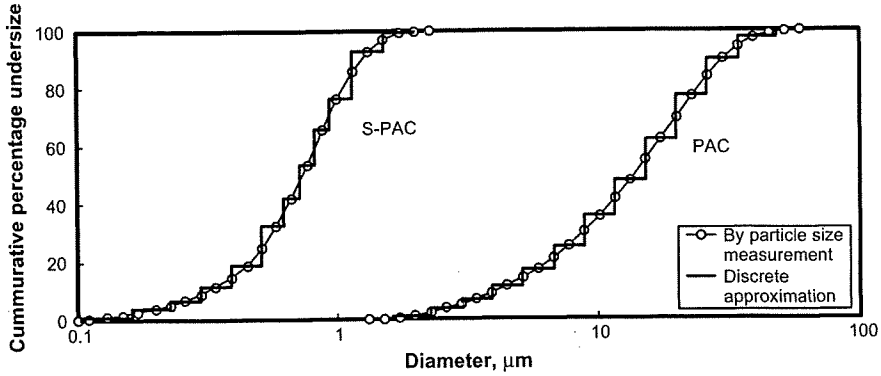

Fig. 4 – Particle size distributions of S-PAC and PAC.

removal was attained within 30 min for S-PAC adsorption, while geosmin removal with PAC was up to only 30% at the same point. With a contact time of 30 min after adding S-PAC, geosmin concentration decreased to 8 ng/L. This is close to the equilibrium concentration, which indicates very fast adsorptive uptake. In contrast, the concentration level attained after 60 min after PAC addition was only half that of its calculated equilibrium. This drastic improvement in geosmin adsorption rate was observed after the activated carbon particle size was reduced to the submicrometer range.

4.2. HSDM simulations

Model simulations were conducted to describe the experimental data on geosmin concentration decay. First HSDM was applied. The particle size distributions of S-PAC and PAC were each represented by 13 discrete particle size classes, as shown in Fig. 4, but one single D_S was used for the 13 discrete particle size class. The model parameters for the Freundlich equation, obtained from isotherm data independently of adsorption kinetic data, were used for both S-PAC and PAC. Mass transfer resistance across the liquid film external to adsorbent particle surfaces was substantially neglected because it cannot be the rate-determining step in well mixed reactors (Sontheimer et al., 1988). In model simulations, the liquid film mass transfer coefficient (k_F) was set to 10 cm/s, at which value the liquid film mass transfer did not control geosmin uptake to adsorbent; this was known because using any values larger than 10 cm/s yielded the same simulation results for concentration decay curves. Finally the surface diffusion coefficient D_S, the remaining unknown model parameter in HSDM, was sought by determining the value that produced best fits to the experimental data.

Two HSDM simulations were conducted: Simulation 1 searched one single D_S value to fit each S-PAC and PAC experimental dataset independently, while Simulation 2 searched one single D_S value to fit both S-PAC and PAC experimental datasets. The best fits were obtained with D_S values of 1.5×10^{-13} cm^2/s for S-PAC and 1.6×10^{-12} cm^2/s for PAC in Simulation 1 (solid lines in Fig. 5). A single D_S value (2.9×10^{-13} m^2/s), although optimized to give the best fit, could not describe combined adsorption kinetic data for S-PAC and PAC (Simulation 2; dashed lines in Fig. 5). The fact that much smaller D_S values were needed for S-PAC than for PAC to describe the geosmin concentration changes (Simulation 1) indicates that surface diffusivity is dependent on adsorbent particle size in the particle size range from tens of micrometers down to submicrometer values. This result also argues against using a constant D_S value in HSDM simulations of each data set, because there is a unique particle size distribution for each adsorbent (S-PAC and PAC) and D_S values should be optimized according to particle size.

4.3. BPKM simulations

BPKM was next applied, in which modeling of the radial intraparticle diffusion through macropores is followed by modeling of local mass transfer from macropore to micropore. One single set of kinetic parameters in the BPKM was searched to fit both PAC and S-PAC experimental datasets. The experimental data for geosmin concentration decay curves of both S-PAC and PAC were well simulated by BPKM using the same set of kinetic parameter values (Fig. 6). The HSDM with one

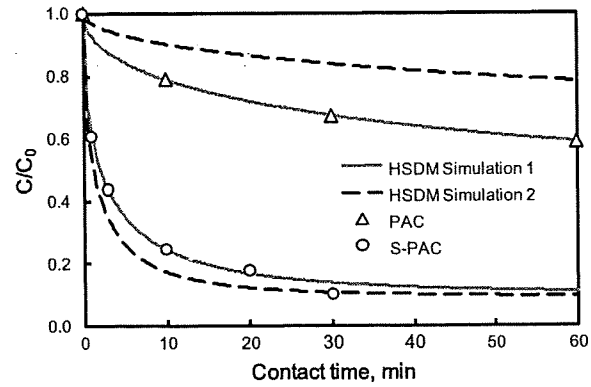

Fig. 5 – Batch adsorption kinetics of geosmin. Solid lines are fit to observed data and dashed lines are simulations by HSDM. Initial geosmin concentrations were 78 and 98 ng/L for S-PAC and PAC, respectively. Activated carbon dosage was 0.6 mg/L. Surface diffusivities were 1.5×10^{-13} cm^2/s for S-PAC and 1.6×10^{-12} cm^2/s for PAC in Simulation 1. Surface diffusivities are 2.9×10^{-13} m^2/s for both S-PAC and PAC in Simulation 2.

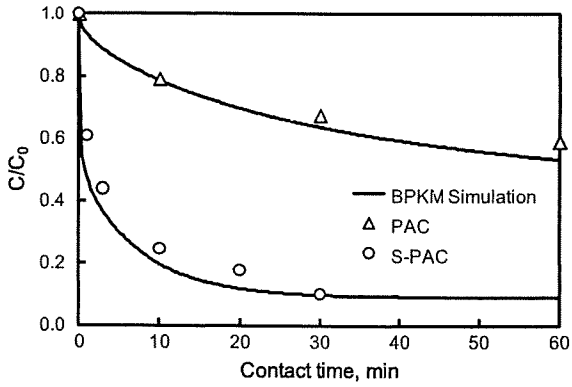

Fig. 6 – Batch adsorption kinetics of geosmin. Points are observed data and lines are simulation by BPKM. Initial geosmin concentrations were 78 ng/L and 98 ng/L for S-PAC and PAC, respectively. Activated carbon dosage was 0.6 mg/L. Surface diffusivity was 5.8×10^{-12} m²/s, rate coefficient for mass transfer between macropore and micropore was 8.3×10^{-4} s^{-1}, and fraction of adsorptive capacity available in macropore region was 0.47.

single D_S value failed to describe the geosmin concentration decay curves of PAC and S-PAC simultaneously (see the previous section "HSDM simulations"). The BPKM can be considered an extended version of HSDM where local mass transfer between macropore and micropore is newly introduced, in addition to the radial diffusion that HSDM has taken into account. In the BPKM, the local mass transfer rate is expressed by the linear driving force model, which implicitly assumes a certain travel distance in the local mass transfer. The successful use of the same rate coefficient value for the local mass transfer between macropore and micropore, which is one of the kinetic parameter values, means the independency of this rate coefficient from adsorbent particle size. Therefore, it implies that travel distance in local mass transfer from macropore to micropore is not different for PAC and S-PAC, and the travel distance could be much shorter than the submicrometer S-PAC particle size.

While radial diffusion is the sole mass transfer resistance and rate-determining step in HSDM, BPKM has two mass transfer resistances. Parameter sensitivity analysis was conducted to identify the mass transport step with most influence in BPKM. One-at-a-time sensitivity measures were made by varying either the surface diffusion coefficient value or the rate coefficient for mass transfer between macropore and micropore for S-PAC and PAC adsorption processes (Fig. 7). In PAC adsorption, D_S affects geosmin removal more than k_B. In S-PAC adsorption, however, k_B is more significant than D_S. High sensitivity to D_S values means the overall rate process is controlled by radial intraparticle diffusion, while high sensitivity to k_B values means it is controlled by local micropore diffusion. The sensitivity analysis indicates that the rate-determining step in overall mass transfer process shifted, from radial intraparticle diffusion to local micropore diffusion, when adsorbent particle size decreased from PAC to S-PAC.

Although it is generally known that smaller adsorbent particle size leads to higher adsorptive removal rate, it is not yet known to what particle size adsorbent should be pulverized, to improve adsorptive removal rate. Adsorbent with particles smaller than a certain size should not be cost-effective. Moreover, the application of pulverization technology raises the question related to the cost-effectiveness issue: to what size should adsorbent particles be pulverized? After the success of the BPKM using a single set of kinetic parameter values, model simulations was conducted to see how adsorbent particle size reduction affects geosmin removal efficiency. In the model simulations, pulverized activated carbon preparations were assumed to have particle size distributions of similar shape to our experimental S-PAC.

BPKM simulation revealed that particle size reduction to 1–2 μm was effective in improving geosmin removal rate, but no further removal enhancement was expected when activated carbon is further pulverized down to less than 1 μm for carbon-water contact times longer than 10 min (Fig. 8). In our experience of pulverization, activated carbon particle diameter was easily reduced to 1 μm but further size reductions were not easily attained and much longer pulverization times were required. There are diminishing marginal returns beyond the 1 μm size. In practical situations, the competitive adsorption effect of NOM (natural organic matter) should be considered: S-PAC adsorbs more NOM and then receives more

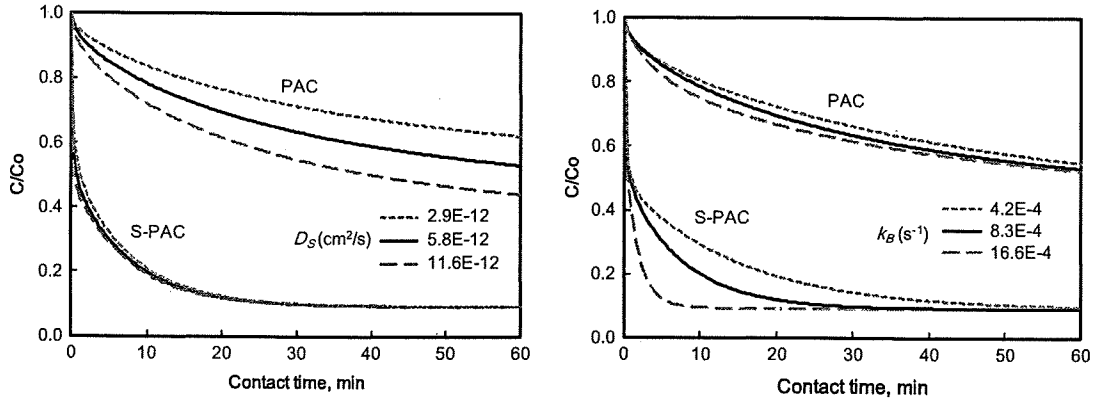

Fig. 7 – Sensitivity analysis to study the effects of D_S (left panel) and k_B (right panel). These values are decreased and increased by a factor of 2 from those of Fig. 6, while holding the other parameter values fixed.

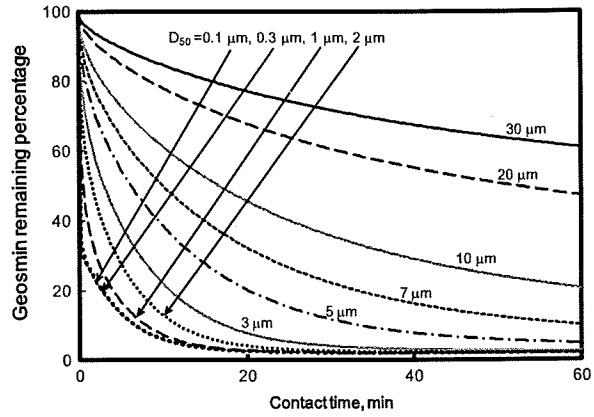

Fig. 8 – Sensitivity analysis to study the effect of activated carbon particle size. Diameter of particles is represented by volume-median diameter, D_{50}. Initial geosmin concentration was 100 ng/L. The parameter values of BPKM are from the same as those of Fig. 6.

competitive adsorption effect (Matsui et al., 2003). Further study is needed to determine the optimum activated carbon particle size, but 1 μm diameter S-PAC is recommended.

5. Conclusions

(1) Adsorption behaviors of geosmin, at 100 ng/L, on S-PAC and PAC in batch reactors, were experimentally observed and mathematically modeled.
(2) No substantial geosmin adsorption capacity difference was observed between S-PAC and PAC. At a given contact time, however, geosmin removal by S-PAC was better than that by PAC.
(3) In HSDM, the intraparticle surface diffusivity for S-PAC was lower than that for PAC. This result indicates the aptitude of BPKM, which additionally incorporates local mass transfer from macropore to micropore.
(4) A numerical solution to the BPKM in batch adsorption systems has been developed using the orthogonal collocation method. The BPKM successfully described adsorption behaviors of geosmin on S-PAC and PAC. In BPKM, the local mass transfer from macropore to micropore controls geosmin adsorption kinetics in S-PAC, while radial macropore diffusion controls in PAC. The BPKM simulations indicate that geosmin removal is improved until activated carbon particle size is below 1 μm, but the merit of particles sizes smaller than 1 μm is small.

Acknowledgements

This study was supported by Grant-in-Aid for Scientific Research B (19360235) from the Ministry of Education, Science, Sports and Culture of the Government of Japan, a research grant from the Ministry of Health, Labor and Welfare, and by Metawater Co., Ltd., Tokyo, Japan.

Appendix A

The particle size distribution of adsorbent was approximated by a discrete density function consisting of M size classes. Eqs. (3),(4),(6),(7), and(8) were rearranged and converted to:

$$\phi\frac{\partial q_{M,i}(t,r)}{\partial t}=\frac{\phi}{r^2}\frac{\partial}{\partial r}\left\{D_S r^2\left[\frac{\partial q_{M,i}(t,r)}{\partial r}\right]\right\}-k_B\left[q_{M,i}(t,r)-q_{B,i}(t,r)\right],\quad i=1,M$$

$$(1-\phi)\frac{\partial q_{B,i}(t,r)}{\partial t}=k_B\left[q_{M,i}(t,r)-q_{B,i}(t,r)\right],\quad i=1,M$$

$$\frac{d}{dt}\left\{\int_0^R\left[\phi q_{M,i}(t,r)+(1-\phi)\times q_{B,i}(t,r)\right]r^2\,dr\right\}\frac{1}{R^2}=\frac{k_F}{\rho}\left[C(t)-c_{l,i}(t)\right],\quad i=1,M$$

$$\frac{dC(t)}{dt}=-\frac{3C_C k_F}{\rho}\sum_{i=1}^{M}\frac{F_i}{R_i}\left[C(t)-c_{l,i}(t)\right],\quad i=1,M$$

$$c_{l,i}(t)=\left[\frac{q_{M,i}(t,R)}{K_F}\right]^{n_F},\quad i=1,M$$

where subscript i denotes size class and M is the total number of size classes, R_i is the radius of an adsorbent particle of the i-th size class, and F_i is the fraction of mass of adsorbent with particle radius R_i.

Usually, BPKM and HSDM are solved using finite difference techniques, such as the Crank-Nicolson method (Peel and Benedek, 1980a,b; McKay and Mckee, 1987; Tien, 1994; Ko et al., 2002, 2003, 2005; Ahn et al., 2005). Orthogonal collocation method, which is simpler for numerical calculation, was, however, applied in this research. Solid phase concentrations, $q_{M,i}(t,r)$ and $q_{B,i}(t,r)$, were expanded in terms of orthogonal polynomials, then the above equations were converted into ordinary differential equations with respect to time, by which the resultant equations can be solved in terms of solution at the collocation points (Villadsen and Stewart, 1967; Friedman, 1984):

$$\phi\frac{dq_{M,i,j}(t)}{dt}=\frac{\phi D_S}{R_i^2}\sum_{k=1}^{N+1}B_{j,k}^{T}q_{M,i,k}(t)-k_B\left[q_{M,i,j}(t)-q_{B,i,j}(t)\right],\quad j=1,N,\quad i=1,M$$

$$(1-\phi)\frac{dq_{B,i,j}(t)}{dt}=k_B\left[q_{M,i,j}(t)-q_{B,i,j}(t)\right],\quad j=1,N+1,\quad i=1,M$$

$$\frac{d}{dt}\sum_{k=1}^{N+1}\left[\phi W_k^{T}q_{M,i,k}(t)+(1-\phi)\times W_k^{T}q_{B,i,k}(t)\right]=\frac{k_F}{\rho R}\left[C(t)-c_{l,i}(t)\right],\quad i=1,M$$

$$\frac{dC(t)}{dt}=-\frac{3C_C k_F}{\rho}\sum_{i=1}^{M}\frac{F_i}{R_i}\left[C(t)-c_{l,i}(t)\right],\quad i=1,M$$

$$c_{l,i}(t)=\left[\frac{q_{M,i,NC}(t)}{K_F}\right]^{n_F},\quad i=1,M$$

where N is the number of collocation points, $B_{j,k}^{T}$ is Laplacian operator matrix, and W_k^{T} is the integral operator vector, which

can be calculated with the algorism described by Villadsen and Stewart (1967).

These equations are rearranged to yield the following equations:

$$\frac{dq_{M,i,j}(t)}{dt} = \frac{D_S}{R_i}\sum_{k=1}^{N+1} B^T_{j,k} q_{M,i,k}(t) - \frac{k_B}{\phi}\left[q_{M,i,j}(t) - q_{B,i,j}(t)\right], \quad j = 1, N, \quad i = 1, M$$

$$\frac{dq_{M,i,N+1}(t)}{dt} = \frac{k_F}{W^T_{NC}\phi\rho R}\left\{C(t) - \left[\frac{q_{M,i,NC}(t)}{K_F}\right]^{n_F}\right\} - \frac{k_B}{\phi}\left[q_{M,i,NC}(t) - q_{B,i,NC}(t)\right] - \sum_{j=1}^{N}\left\langle \frac{W^T_j}{W^T_{NC}}\left\{\frac{D_S}{R_i^2}\sum_{k=1}^{N} B^T_{j,k} q_{M,i,k}(t) - \frac{k_B}{\phi}\left[q_{M,i,j}(t) - q_{B,i,j}(t)\right]\right\} + \frac{W^T_j}{W^T_{NC}}\frac{k_B}{\phi}\left[q_{M,i,j}(t) - q_{B,i,j}(t)\right]\right\rangle \quad i = 1, M$$

$$\frac{dq_{B,i,j}(t)}{dt} = \frac{k_B}{1-\phi}\left[q_{M,i,j}(t) - q_{B,i,j}(t)\right], \quad j = 1, N+1, \quad i = 1, M$$

$$\frac{dC(t)}{dt} = -\frac{3C_C k_F}{\rho}\sum_{i=1}^{M}\frac{F_i}{R_i}\left\{C(t) - \left[\frac{q_{M,i,NC}(t)}{K_F}\right]^{n_F}\right\}$$

The above $[(N+1)\times M+1]$ equations were integrated as a system of ordinary differential equations by the Gear's stiff method (backward differentiation formulas) with analytical Jacobian as given in the IMSL Math Library. The Gear's stiff method requires the Jacobian matrix of a given set of independent variables. Since the problem of the equation is extremely stiff, analytical Jacobian equations, instead of the numerical Jacobian, were inevitable in solving these stiff differential equations in stable. The Jacobian equations are easily derived from the equations (not shown in this paper). For the model simulations in this paper, N was 11 and M was 13.

REFERENCES

Ahn, S., Werner, D., Karapanagioti, H.K., McGlothlin, D.R., Zare, R.N., Luthy, R.G., 2005. Phenanthrene and pyrene sorption and intraparticle diffusion in polyoxymethylene, coke, and activated carbon. Environ. Sci. Technol. 39 (17), 6516–6526.

Buchholz, H., Krückels, W., 1976. Sorptionskinetik gelöster organischer substanzen an aktivkohlen. Verfahrenstechnik 10 (5), 290–296.

Chang, C.-F., Chang, C.-Y., Höll, W., Ulmer, M., Chen, Y.-H., Groß, H.-J., 2004. Adsorption kinetics of polyethylene glycol from aqueous solution onto activated carbon. Water Res. 38 (10), 2559–2570.

Cook, D., Newcombe, G., Sztajnbok, P., 2001. The application of powdered activated carbon. Water Res. 35 (5), 1325–1333.

Friedman, G., 1984. Mathematical modeling of multicomponent adsorption in batch and fixed-bed reactors, MS Thesis, Michigan Technological Univ. Ann Arbor, Michigan, USA.

Graham, M.R., Summers, R.S., Simpson, M.R., MacLeod, B.W., 2000. Modeling equilibrium adsorption of 2-methylisoborneol and geosmin in natural waters. Water Res. 34 (8), 2291–2300.

Jia, Q., Lua, A.C., 2008. Concentration-dependent branched pore kinetic model for aqueous phase adsorption. Chem. Eng. J. 136, 227–235.

Ko, D.C.K., Porter, J.F., McKay, G., 2002. A branched pore model analysis for the adsorption of acid dyes on activated carbon. Adsorption 8 (3), 171–188.

Ko, D.C.K., Tsang, D.H.K., Porter, J.F., McKay, G., 2003. Applications of multipore model for the mechanism identification during the adsorption of dye on activated carbon and bagasse pith. Langmuir 19 (3), 722–730.

Ko, D.C.K., Cheung, C.W., Porter, J.F., 2005. A branched pore kinetic model applied to the sorption of metal ions on bone char. J. Chem. Technol. Biotechnol. 80 (8), 861–871.

Lalezary-Craig, S., Pirbazari, M., Dale, M.S., Tanaka, T.S., McGuire, M.J., 1988. Optimizing the removal of geosmin and 2-methylisoborneol by powdered activated carbon. J. Am. Water Works Assoc. 80 (3), 73–80.

Lua, A.C., Jia, Q.P., 2007. Adsorption of phenol by oil-palm-shell activated carbons. Adsorption 13 (2), 129–137.

Mallevialle, J., Suffet, I.H., 1987. Identification and Treatment of Tastes and Odors in Drinking Water. American Water Works Association, Denver, CO, USA.

Matsui, Y., Fukuda, Y., Inoue, T., Matsushita, T., 2003. Effect of natural organic matter on powdered activated carbon adsorption of trace contaminants: characteristics and mechanism of competitive adsorption. Water Res. 37 (18), 4413–4424.

Matsui, Y., Fukuda, Y., Murase, R., Aoki, N., Mima, S., Inoue, T., Matsushita, T., 2004. Micro-ground powdered activated carbon for effective removal of natural organic matter during water treatment. Water Sci. Tech.: Water Supply 4 (4), 155–163.

Matsui, Y., Aizawa, T., Kanda, F., Nigorikawa, N., Mima, S., Kawase, Y., 2007. Adsorptive removal of geosmin by ceramic membrane filtration with super-powdered activated carbon. J. Water Supply: Res. Technol. -AQUA 56 (6–7), 411–418.

Matsui, Y., Murai, K., Sasaki, H., Ohno, K., Matsushita, T., 2008. Submicron-sized activated carbon particles for the rapid removal of chlorinous and earthy-musty compounds. J. Water Supply: Res. Technol. -AQUA 57 (8), 577–583.

McGuire, M.J., Krasner, S.W., Hwang, C.J., Izaguirre, G., 1981. Closed-loop stripping analysis as a tool for solving taste and odor problems. J. Am. Water Works Assoc. 73 (10), 530–537.

McKay, G., Mckee, S., 1987. Solid-liquid adsorption based on external mass transfer, macropore and micropore diffusion. Chem. Eng. Sci. 42 (5), 1145–1151.

Najm, I.N., Snoeyink, V.L., Suidan, M.T., Lee, C.H., Richard, Y., 1990. Effect of particle size and background natural organics on the adsorption efficiency of PAC.J. Am. Water Works Assoc. 82 (1), 65–72.

Newcombe, G., Drikas, M., Hayes, R., 1997. Influence of characterised natural organic material on activated carbon adsorption .2. Effect on pore volume distribution and adsorption of 2-methylisoborneol. Water Res. 31 (5), 1065–1073.

Peel, R.G., Benedek, A., 1980a. Attainment of equilibrium in activated carbon isotherm studies. Environ. Sci. Technol. 14 (1), 66–71.

Peel, R.G., Benedek, A., 1980b. Dual rate kinetic model of fixed bed adsorber. J. Environ. Eng.-ASCE 106 (4), 797–813.

Sontheimer, H., Crittenden, J.C., Summers, R.S., 1988. Activated Carbon for Water Treatment, 2nd ed. DVGW-Forschungsstelle, Karlsruhe, Germany.

Tien, C., 1994. Adsorption Calculations and Modeling. Butterworth-Heinemann, Boston, USA.

Traegner, U.K., Suidan, M.T., Kim, B.R., 1996. Considering age and size distributions of activated-carbon particles in